JPET Fast Forward. Published on May 27, 2020 as DOI: 10.1124/jpet.120.266023
This article has not been copyedited and formatted. The final version may differ from this version.

[^{3}H]Dopamine Uptake through the Dopamine and Norepinephrine Transporters is Decreased in the Prefrontal Cortex of Transgenic Mice Expressing HIV-1 Tat Protein

Matthew Strauss, Bernadette O'Donovan, Yizhi Ma, Ziyu Xiao, Steven Lin, Michael T. Bardo, Pavel I. Ortinski, Jay P. McLaughlin, and Jun Zhu*

MS, YM, ZX, SL, JZ - Department of Drug Discovery and Biomedical Sciences, College of Pharmacy, University of South Carolina, Columbia, SC 29208 USA

BO - Department of Physiology, Pharmacology and Neuroscience, School of Medicine, University of South Carolina, Columbia, SC 29208 USA

MB - Department Psychology, University of Kentucky, Lexington, KY 40536 USA

PO – Department of Neuroscience, University of Kentucky, Lexington, KY 40536, USA

JM - Department of Pharmacodynamics, College of Pharmacy, University of Florida, Gainesville, FL 32611 USA

JPET Fast Forward. Published on May 27, 2020 as DOI: 10.1124/jpet.120.266023
This article has not been copyedited and formatted. The final version may differ from this version.

DA uptake via DAT and NET is reduced in the PFC of iTat mice

Corresponding Author:
Jun Zhu, MD, PhD
Department of Drug Discovery and Biomedical Sciences
College of Pharmacy
University of South Carolina
715 Sumter Street, Columbia, SC 29208, USA.
Tel: +1-803-777-7924; Fax: +1-803-777-8356
E-mail: zhuj@cop.sc.edu

Number of:

Text pages: 38
Tables: 1
Figures: 5
References: 88

Number of words in:

Abstract: 250
Introduction: 729
Discussion: 1827

Running Title: *In vivo* Tat expression reduces DAT and NET in the mouse PFC

Nonstandard abbreviations:
DA – Dopamine
DAT – Dopamine transporter
HAND – HIV-associated neurocognitive disorder
HIP – Hippocampus
iTat-tg – inducible tat transgenic mouse
NE – Norepinephrine
NET – Norepinephrine transporter
PFC – prefrontal cortex
STR – Striatum

Recommended section assignment:
Neuropharmacology

JPET Fast Forward. Published on May 27, 2020 as DOI: 10.1124/jpet.120.266023
This article has not been copyedited and formatted. The final version may differ from this version.

Abstract

Dysregulation of dopamine neurotransmission has been linked to the development of HIV-1 associated neurocognitive disorders (HAND). To investigate the mechanisms underlying this phenomenon, this study utilized an inducible HIV-1 transactivator of transcription (Tat) transgenic (iTat-tg) mouse model, which demonstrates brain-specific Tat expression induced by administration of doxycycline. We found that induction of Tat expression in the iTat-tg mice for either 7 or 14 days resulted in a decrease (~30%) in the V_{max} of [^{3}H]DA uptake via both the dopamine transporter (DAT) and norepinephrine transporter (NET) in the prefrontal cortex (PFC), which was comparable to the magnitude (~35%) of the decrease in B_{max} for [^{3}H]WIN 35,428 and [^{3}H]Nisoxetine binding to DAT and NET, respectively. The decreased V_{max} was not accompanied by a reduction of total or plasma membrane expression of DAT and NET. Consistent with the decreased V_{max} for DAT and NET in the PFC, the current study also found an increase in the tissue content of DA and dihydroxyphenylacetic acid (DOPAC) in the PFC of iTat-tg mice following 7-day administration of doxycycline. Electrophysiological recordings in layer V pyramidal neurons of the prelimbic cortex from iTat-tg mice found a significant reduction in action potential firing, which was not sensitive to selective inhibitors for DAT and NET, respectively. These findings provide a molecular basis for using the iTat-tg mouse model in the studies of NeuroHIV. Determining the mechanistic basis underlying the interaction between Tat and DAT/NET may reveal novel therapeutic possibilities for preventing the increase in comorbid conditions as well as HAND.

JPET Fast Forward. Published on May 27, 2020 as DOI: 10.1124/jpet.120.266023
This article has not been copyedited and formatted. The final version may differ from this version.

Significance Statement

HIV-1 infection disrupts dopaminergic neurotransmission, leading to HIV-1 associated neurocognitive disorders. Based on our *in vitro* and *in vivo* studies, dopamine uptake via both dopamine and norepinephrine transporters is decreased in the prefrontal cortex of HIV-1 Tat transgenic mice, which is consistent with the increased dopamine and DOPAC contents in this brain region. Thus, these plasma membrane transporters are an important potential target for therapeutic intervention for patients with HAND.

JPET Fast Forward. Published on May 27, 2020 as DOI: 10.1124/jpet.120.266023
This article has not been copyedited and formatted. The final version may differ from this version.

Introduction

Acquisition of the Human Immunodeficiency Virus (HIV) leads to the development of acquired immunodeficiency syndrome (AIDS) and continues to be a global public health problem, with an estimated 37 million HIV-1 positive individuals worldwide. Despite the success of combinatorial antiretroviral therapy (cART) in controlling peripheral HIV infection and improving the life of HIV patients, roughly 50% of HIV-1 patients develop a group of neurological complications including cognitive dysfunction, motor deficits, and dementia collectively referred to as HIV-associated neurocognitive disorders (HAND) (Heaton et al., 2010). Persistent viral replication and expression of HIV-1 viral proteins within the CNS are central to the development of HAND (Gaskill et al., 2009), particularly since most cART medications cannot cross the blood-brain barrier, while infected macrophages carrying the virus can (Buckner et al., 2006). Considering long-term viral protein exposure can accelerate damage to the mesocorticolimbic dopamine (DA) system (Nath et al., 1987; Berger and Arendt, 2000; Koutsilieri et al., 2002), there is a pressing need to define the molecular mechanism(s) by which HIV-1 infection impairs the DA system and affects the progression of HAND. HIV-1 viral proteins are associated with the persistence of HIV-related neuropathology and subsequent neurocognitive deficits (Frankel and Young, 1998; Power et al., 1998; Brack-Werner, 1999; Johnston et al., 2001). Specifically, the continuing presence of the transactivator of transcription (Tat) protein in CART-treated HIV patients (Johnson et al., 2013; Henderson et al., 2019), may play a crucial role in the neurotoxicity and cognitive impairment evident in neuroAIDS (Rappaport et al., 1999; King et al., 2006), as the HIV-1 Tat protein has been detected in DA-rich brain areas (Del Valle et al., 2000; Hudson et al., 2000; Lamers et al., 2010) and in the sera (Westendorp et al., 1995; Xiao et al., 2000) of HIV-1 infected patients (Johnson et al., 2013).

Maintaining a normal physiological DA system is essential for a variety of brain activities involved in attention, learning, memory (Nieoullon, 2002; Cools, 2006), and motivation (Lammel et al., 2012; Tye et al., 2013). Converging lines of clinical observations, supported by imaging

JPET Fast Forward. Published on May 27, 2020 as DOI: 10.1124/jpet.120.266023
This article has not been copyedited and formatted. The final version may differ from this version.

(Wang et al., 2004; Chang et al., 2008), neuropsychological performance testing (Kumar et al., 2011; Meade et al., 2011), and postmortem examinations (Gelman et al., 2012), have demonstrated that DA dysregulation is correlated with the abnormal neurocognitive function observed in HAND (Berger and Arendt, 2000; Purohit et al., 2011). Therapy-naïve HIV patients demonstrate increased levels of DA and decreased DA turnover in the early stages of HIV infection (Scheller et al., 2010), which may initiate compensatory mechanisms eventually resulting in decreased DA levels (Sardar et al., 1996; Kumar et al., 2009; Kumar et al., 2011) and dopaminergic neuron damage (Wang et al., 2004; Chang et al., 2008) in the advanced stages of HIV infection.

DA transporter (DAT)-mediated DA reuptake is critical for maintaining normal DA homeostasis. Human DAT (hDAT) activity is strikingly reduced in HIV-1-infected patients, particularly those with a history of cocaine abuse, correlating with the severity of HIV-1 associated cognitive deficits (Wang et al., 2004; Chang et al., 2008). Our published *in vitro* work has demonstrated that exogenous application of recombinant Tat_{1-86} protein decreases DAT activity in cells (Midde et al., 2013; Midde et al., 2015; Quizon et al., 2016) and rat brain synaptosomes (Zhu et al., 2009b). This research raises a critical question of whether the *in vitro* Tat-dysregulated DAT function can be replicated with *in vivo* biological expression of Tat protein in an animal model, which may contribute to the neurocognitive deficits observed in both these animals and HIV infected individuals. Moreover, the prefrontal cortex is an important brain region for higher cognitive function, where not only the DAT but also the norepinephrine (NE) transporter (NET) is capable of DA reuptake (Moron et al., 2002). For this reason, it is possible that Tat-induced dysfunction of DA system could be mediated by inhibition of both DAT and NET. The inducible Tat transgenic (iTat-tg) mouse model recapitulates many aspects of the neuropathologies and neurocognitive impairments observed in HAND (Kim et al., 2003) and represents clinically relevant model of symptomatic NeuroHIV. Thus, investigating the neuropathogenic role of DAT/NET-mediated dopaminergic transmission in the brain of iTat-tg

JPET Fast Forward. Published on May 27, 2020 as DOI: 10.1124/jpet.120.266023
This article has not been copyedited and formatted. The final version may differ from this version.

mice may provide mechanistic insight into the development of cognitive deficits in HIV-1 infected population. This iTat-tg mouse model allows for determination of how *in vivo* Tat protein expression influences dopaminergic neurotransmission by inhibiting DAT and NET, which may contribute to the development of HAND.

JPET Fast Forward. Published on May 27, 2020 as DOI: 10.1124/jpet.120.266023
This article has not been copyedited and formatted. The final version may differ from this version.

Materials and Methods

Animals

Male iTat-tg and G-tg mice breeding stock were provided by Dr. Jay P. McLaughlin at the University of Florida College of Pharmacy (Gainesville, FL). Mice in this colony were established from progenitors originally derived by Dr. Johnny J. He (Kim et al., 2003), at the Rosalind Franklin University of Medicine and Science (Chicago, IL). The iTat-tg mouse line genetically expresses a "tetracycline-on (TETON)" system, which is integrated into the regulator for the astrocyte-specific glial fibrillary acidic protein (GFAP) promoter and coupled to the Tat_{1-86} coding gene, allowing astrocyte (brain)-specific Tat_{1-86} expression induced by doxycycline (Dox) administration (Kim et al., 2003). The iTat-tg mouse model facilitates the needed focus on Tat protein, allowing us to study Tat-mediated dysregulation of DAT and NET. In contrast, the G-tg mice possess the TETON system integrated into GFAP but lack the Tat_{1-86} coding gene, rendering them incapable of Tat expression, but highly suitable as control subjects. Since the iTat-tg and G-tg mice are developed from C57BL/6J mouse strain, C57BL/6J mice (obtained from the Jackson Laboratory, Bar Harbor, ME) were used as another control mouse line. Mice used for all experiments were between the age of 9-14 weeks (see Supplemental Table 4). This age range was chosen based on the previous reports which found both physiological (Carey et al., 2013; Cirino et al., 2020) and behavioral deficits (Carey et al., 2012; Paris et al., 2014; Paris et al., 2015) in the iTat-tg mice using an identical age range. At the completion of all experiments, we conducted the correlation analysis on the age with the respective experimental data values from individual animals following 7- or 14-day administration of Dox, which revealed no correlation between age and the respective experimental data values (see Supplemental Table 5). Mice were housed (4-5 mice/cage) in a temperature (21 ± 2 °C)- and humidity (50 ± 10%)-controlled vivarium, which were maintained on a 12:12 h light/dark cycle (lights on at 07:00 h) with ad libitum access to food and water. Animals were maintained in accordance with the Guide for the Care and Use of Laboratory Animals under the National Institute of Health

JPET Fast Forward. Published on May 27, 2020 as DOI: 10.1124/jpet.120.266023
This article has not been copyedited and formatted. The final version may differ from this version.

(NIH) guidelines in the Assessment and Accreditation of Laboratory Animal Care accredited facilities. The experimental protocol was approved by the Institutional Animal Care and Use Committee (IACUC) at the University of South Carolina, Columbia.

Drug administration and Synaptosomal preparation

Male iTat-tg, G-tg, and C57BL/6J mice were administered either Dox (100 mg/kg/day, Sigma-Aldrich; St. Louis, MO) or saline (10 µl/gram body weight) via intraperitoneal injection for 7 or 14 consecutive days. The optimized dose of Dox was chosen because it has been previously proven efficacious for induction of Tat (Zou et al., 2007; Carey et al., 2012; Paris et al., 2014b) and findings showing that iTat so induced is biologically active during the period of behavioral testing (Zou et al., 2007). The 7- or 14-Dox or saline treatment paradigm was chosen for the kinetic analysis of DA uptake based on the previous behavior studies (Carey et al., 2012; Carey et al., 2013; Paris et al., 2014a). In addition, based on the previous report showing no significant difference in Tat immunoreactivity in whole brain of iTat-tg mice following 7- or 14-day administration of Dox (Paris et al., 2014b), and because no difference in the inhibitory effects of Tat on DA uptake were observed between these time points, only 7-day administration paradigm was used in the subsequent studies. Selection of animals for saline or Dox treatment was made randomly among littermates.

All mice were rapidly decapitated 24 h after last saline or Dox injection. Brain tissue dissected from prefrontal cortex (PFC, prelimbic and infralimbic cortices combined), striatum, and hippocampus was pooled from a group of three mice (constituting a single sample for each region), which was used as a single replicate (*n*) for conducting independent experiments. Thus, "*n*" refers the number of independent experiments conducted, rather than the number of mice used. Synaptosomes were prepared using our published method (Zhu et al., 2004). The PFC region was a focus of the current study because it is a critical brain region for higher cognitive function (Miller and Cohen, 2001; Dalley et al., 2004; Ridderinkhof et al., 2004), where the NET

JPET Fast Forward. Published on May 27, 2020 as DOI: 10.1124/jpet.120.266023
This article has not been copyedited and formatted. The final version may differ from this version.

also plays a role in DA uptake (Horn, 1973a; Raiteri et al., 1977). Given that DA uptake through DAT or NET is not identical throughout various brain regions, the DA uptake through DAT in striatum and NET in hippocampus were examined in addition to the PFC. The striatum and hippocampus were also selected due to their central role in DA neurotransmission (Horn, 1973b; Raiteri et al., 1977; Borgkvist et al., 2012). The tissue was homogenized immediately in 20 mL of ice-cold 0.32 M sucrose buffer containing 2.1 mM of NaH_2PO_4 and 7.3 mM of Na_2HPO_4, pH 7.4; with 16 up-and-down strokes using a Teflon pestle homogenizer (clearance approximately 0.003 in.). Homogenates were centrifuged at 1,000g for 10 min at 4°C and the resulting supernatants were then centrifuged at 12,000g for 20 min at 4°C. The resulting pellets were resuspended in the respective buffer for each individual assay as noted below.

Kinetic analysis of synaptosomal [^{3}H]DA uptake assay

To determine whether Dox-induced biological Tat expression alters DA uptake via DAT or NET, the maximal velocity (V_{max}) and Michaelis-Menten constant (K_m) of synaptosomal [^{3}H]DA uptake were examined using a previously described method (Zhu et al., 2016). In a pilot study, we measured the synaptosomal [^{3}H]DA uptake via DAT, NET, or the serotonin transporter (SERT) in whole C57BL/6J mouse brain with the utilization of selective inhibitors for the individual transporters and found that the portion of DA uptake via DAT, NET or SERT is 80%, 17%, and 3%, respectively (data not shown). Due to the minimal level of DA uptake via SERT, this transporter was not examined in the current study. Importantly, although NET density is overall lower in the whole mouse brain, in the PFC the NET is more concentrated than the DAT and plays a primary role in reuptake of DA (Moll et al., 2000; Moron et al., 2002), and thus warranted the present investigation. Because DA is transported by DAT, NET, and SERT in the PFC (Moron et al., 2002; Williams and Steketee, 2004), kinetic analysis of [^{3}H]DA uptake via DAT in the PFC was assessed in the presence of desipramine (1 uM) and paroxetine (5 nM) to prevent DA uptake into norepinephrine- and serotonin-containing nerve terminals,

JPET Fast Forward. Published on May 27, 2020 as DOI: 10.1124/jpet.120.266023
This article has not been copyedited and formatted. The final version may differ from this version.

respectively, whereas [^{3}H]DA uptake via NET in the PFC was assessed in the presence of GBR12909 (100 nM) and fluoxetine (100 nM) to prevent DA uptake into dopaminergic- and serotonin-containing nerve terminals, respectively. In brief, the resulting pellets described above were resuspended in Krebs-Ringer-HPES assay buffer (125 mm NaCl, 5 mm KCl, 1.5 mm $MgSO_4$, 1.25 mm $CaCl_2$, 1.5 mm KH_2PO_4, 10 mm glucose, 25 mm HEPES, 0.1 mm EDTA, 0.1 mm pargyline and 0.1 mm L-ascorbic acid, saturated with 95% O_2／5% CO_2, pH 7.4). Aliquots of synaptosomal tissue (50 µg/25 µL) were incubated with one of 6 mixed [^{3}H]DA concentrations containing a range of DA (Sigma-Aldrich; St. Louis, MO) concentrations (1 nM - 5 µM) and fixed [^{3}H]DA (12 nM, Perkin Elmer; Waltham, MA) for 8 minutes at 37 °C. Incubation was terminated by the addition of 3 mL of ice-cold assay buffer, followed by immediate filtration through Whatman GF/B glass fiber filters (presoaked with 1 mM pyrocatechol for 3 h). Filters were washed three times with 3 mL of ice-cold assay buffer using a Brandel cell harvester (Model MP-43RS; Biochemical Research and Development Laboratories Inc., Gaithersburg, MD). Radioactivity was determined by liquid scintillation spectrometry (Model B1600TR, Packard Corporation Inc., Meriden, CT). Bovine serum albumin (Sigma-Aldrich; St. Louis, MO) was used as a standard (Bradford, 1976) to measure protein concentration for all samples. Nonspecific uptake of [^{3}H]DA into DAT or NET was determined in the presence of 10 µM nomifensine (Sigma-Aldrich; St. Louis, MO) or 10 µM desipramine, respectively.

[^{3}H]WIN 35,428 and [^{3}H]Nisoxetine binding assays

[^{3}H]WIN 35,428 and [^{3}H]Nisoxetine (both purchased from Perkin Elmer; Waltham, MA) represent substrate binding sites on the DAT and the NET, respectively. To determine whether biological HIV-1 Tat expression alters these substrate binding sites, we performed the saturation binding of [^{3}H]WIN 35,428 and [^{3}H]Nisoxetine for DAT and NET, respectively, using a previously described method (Reith et al., 2005; Zhu et al., 2009a). Saturation binding assays were conducted in duplicate in a final volume of 250 µL for PFC, striatum, and hippocampus. For

JPET Fast Forward. Published on May 27, 2020 as DOI: 10.1124/jpet.120.266023
This article has not been copyedited and formatted. The final version may differ from this version.

[^{3}H]WIN 35,428 binding, 50 µL aliquots (50 µg protein) of synaptosomes were incubated in 0.32M sucrose buffer (pH: 7.4) containing 2.1 mM NaH_2PO_4 and 7.3 mM Na_2HPO_4 (chemicals purchased from Sigma-Aldrich; St. Louis, MO) with six concentrations of [^{3}H]WIN 35,428 (1, 5, 10, 15, 25, 30 nM) on ice for 2 h. Desipramine (1 µM) was included to inhibit [^{3}H]WIN 35,428 binding to the NET in the PFC. Nonspecific binding was determined in the presence of 10 µM cocaine in the striatum and 10 µM nomifensine in the PFC. For [^{3}H]Nisoxetine binding, 50 µL aliquots (50 µg protein) of synaptosomes were incubated in assay buffer (150 mM Na_2HPO_4, 300 mM NaH_2PO_4, 1.22 M NaCl, 50 mM KCl, 12 mM $MgSO_4$, 100 mM glucose, 10 mM CaCl, and 1 µM EDTA; pH: 7.4) with one of six Nisoxetine concentrations (0.5-30 nM) that was mixed with a fixed concentration of [^{3}H]Nisoxetine (3 nM) on ice for 2 h. 0.1 µM GBR 12909 was included to inhibit [^{3}H]Nisoxetine binding to the DAT. Non-specific binding was determined in the presence of 10 µM desipramine. The reaction was terminated by rapid filtration onto Whatman GF/B glass filter filters, presoaked for 2 h with assay buffer containing 10% polyethylenimine, through a Brandel cell harvester (Model MP-43RS; Biochemical Research and Development Laboratories Inc., Gaithersburg, MD). Filters were washed three times with 3 mL of ice-cold assay buffer. Radioactivity was determined by liquid scintillation spectrometry (Model B1600TR, Packard Corporation Inc., Meriden, CT), and bovine serum albumin (Sigma-Aldrich; St. Louis, MO) was used as a standard (Bradford, 1976) to measure protein concentration for all samples.

Biotinylation and Western Blot Assay.

Biotinylation was performed to determine alterations in plasmalemmal surface expression of DAT in the PFC and striatum and NET in the PFC and hippocampus following Dox-induced Tat expression. Following 7-day administration of Dox or saline, synaptosomes were prepared as described above. The biotinylation assay was performed as described previously (Zhu et al., 2009a). Synaptosomes (800 µg/sample) prepared freshly were incubated in 500 µL of PBS Ca/Mg buffer (138 mM NaCl, 2.7 mM KCl, 1.5 mM KH_2PO_4, and 9.6 mM

JPET Fast Forward. Published on May 27, 2020 as DOI: 10.1124/jpet.120.266023
This article has not been copyedited and formatted. The final version may differ from this version.

Na_2HPO_4; with 1 mM $MgCl_2$ and 0.1 mM $CaCl_2$; Sigma-Aldrich; St. Louis, MO) containing 1.5 mg/mL EZ-link sulfo-NHS-biotin at 4 °C for 1 h. After incubation, samples were centrifuged at 8000g for 4 min at 4 °C. To remove the free sulfo-NHS-biotin, the resulting pellets were resuspended and centrifugated three times with 1 mL of ice-cold 100 mM glycine in PBS/Ca/Mg buffer and centrifugated at 8000g for 4 min at 4 °C. Final resulting pellets were resuspended in 1 mL of ice-cold 100 mM glycine in PBS/Ca/Mg buffer and incubated with continual shaking for 30 min at 4 °C. Samples were centrifuged subsequently at 8000g for 4 min at 4°C, the resulting pellets were resuspended in 1 ml of ice-cold PBS/ Ca/Mg buffer, and the resuspension and centrifugation step were repeated twice. Final pellets were lysed by sonication for 2 to 4 seconds in 500 µL of Triton X-100 buffer (10 mM Tris, 150 mM NaCl, 1 mM EDTA, 1.0% Triton X-100, 1 µg/ml aprotinin, 1 µg/ml leupeptin, 1 µM pepstatin, 250 µM phenylmethysulfonyl fluoride, pH 7.4), followed by incubation and continual shaking for 20 min at 4°C. Lysates were centrifuged at 21,000g for 20 min at 4°C. Pellets were discarded, and 100 µL of supernatant was saved for assessing total DAT or NET expression. Monomeric avidin beads (100 µL, Thermo Scientific; Waltham, MA) were added to the remaining supernatant and incubated for one hour at room temperature. The samples were then centrifuged at 17,000g for 4 min, and 100 µL of the resulting supernatant was saved for the intracellular (non-biotinylated) fraction. Resulting pellets containing the avidin-absorbed biotinylation proteins (cell surface fraction) were resuspended in 1mL of 1.0% Triton X-100 buffer and centrifuged at 17,000g for 4 min at 4°C, which was repeated twice. Final pellets containing the biotinylated DAT and NET absorbed to monomeric avidin beads were eluted by addition of 50 µL of laemmeli buffer (Sigma-Aldrich; St. Louis, MO) and incubated for 20 min at room temperature. The total, intracellular and surface fractions were stored at -20 °C until Western blot assay.

To obtain immunoreactive DAT and NET protein in total synaptosomal, intracellular, and cell surface fractions, samples were thawed and subjected to gel electrophoresis and western blotting. Samples were separated by 10% SDS-polyacrylamide gel electrophoresis for ~90 min

JPET Fast Forward. Published on May 27, 2020 as DOI: 10.1124/jpet.120.266023
This article has not been copyedited and formatted. The final version may differ from this version.

at 125V. Samples were then transferred to Immobilon-P transfer membranes (0.45 µm pore size; Millipore Co., Bedford MA, USA) in transfer buffer (50 mM Tris, 250 mM glycine, 3.5 mM SDS) using a Mini Trans-Blot Electrophoretic Transfer Cell (Bio-Rad; Hercules, CA) for 90 min at 75 V. The membranes were then incubated with blocking buffer (5% milk powder in PBS containing 0.5% Tween-20) for 1 h at room temperature, followed by incubation with either goat anti-DAT (Santa Cruz, C-20 polyclonal antibody, diluted 1:500 in blocking buffer) or mouse anti-NET (MAb tech, 05-1 monoclonal antibody, diluted 1:5,000 in blocking buffer) overnight at 4 °C. Transfer membranes were then washed three times with blocking buffer at room temperature followed by incubation with either anti-goat-HRP (Jackson Laboratory, catalog number 305-035-045 diluted 1:10,000 in blocking buffer) or anti-mouse-HRP (Cell Signaling, catalog number 7076S diluted 1:15,000 in blocking buffer) for 1 h at room temperature. Membranes were then washed an additional three times in PBS containing 0.5% Tween-20 (Sigma-Aldrich; St. Louis, MO). Immunoreactive proteins on the transfer membranes were detected using Amersham ECL prime western blotting detection reagent (GE life sciences; Chicago, IL) and developed on Hyperfilm (GE life sciences; Chicago, IL). After detection and quantification of DAT or NET each blot was washed and re-probed with rabbit anti-Calnexin (Santa Cruz, Biotechnology, catalog number SC-11397 polyclonal antibody, diluted 1:10,000 in blocking buffer), an endoplasmic reticular protein, to monitor protein loading between all groups. Multiple autoradiographs were obtained using different exposure times, and immunoreactive bands within the linear range of detection were quantified by densitometric scanning using Scion image software. Band density measurements, expressed as relative optical density, were used to determine levels of DAT and NET in the total synaptosomal fraction, the intracellular fraction (non-biotinylated), and the cell surface fraction (biotinylated).

HPLC analysis of DA and dihydroxyphenylacetic acid (DOPAC) tissue contents in brain regions

JPET Fast Forward. Published on May 27, 2020 as DOI: 10.1124/jpet.120.266023
This article has not been copyedited and formatted. The final version may differ from this version.

Concentrations of DA and DOPAC in PFC, nucleus accumbens, and striatum in iTat-tg and G-mice following 7-day administration of saline or Dox were determined using a high performance liquid chromatography (HPLC) system coupled with electrochemical detection (HPLC–EC) as described previously (Zhu et al., 2004). Twenty-four hours after the last injection of saline or Dox, whole brains from individual mice were removed and immediately stored in liquid nitrogen, and then stored at −80° C. To prepare samples for HPLC assay, whole brains were sliced on top of an ice-cold plate and brain regions were dissected by biopsy punches with a plunger system (Miltex). Brain tissues were individually stored in 10 volume/tissue weight of 0.1 N perchloric acid at −80° C until assay. Upon assay, samples were thawed on ice, sonicated and centrifuged at 30,000 × g for 15 min at 4° C. For each sample, 20 µl of the resulting supernatant was injected onto the HPLC system. Chromatograms were recorded using EZ Chrom Elite software (Agilent, Santa Clara, CA). Retention times of DA and DOPAC standards were used to identify respective peaks. Peak heights were used to calculate the detected amounts of DA and DOPAC based on a standard curve generated from external standards. The HPLC–EC system (Coulochem III, ThermoFisher Scientific, Columbia MD) consisted of a 582 solvent delivery system, an autosampler (Model 542), a reverse phase HPLC column (MD-150, 3.2 x 150 mm, 3µm, product no 70-0636) and electrochemical detector (cell 5014B). The mobile phase contained 124 mM citric acid monohydrate, 50 mM Na_2HPO_4, 10 mM NaCl, 0.1 mM EDTA, 0.2% octylsulfonic acid–sodium salt and 5% methanol (pH 3.0), using a flow rate of 0.5 ml/min. Samples were kept at 4^o C in a cooling tray in the autosampler.

Patch-clamp Electrophysiology

iTat and C57 mice were decapitated following isoflurane anesthesia 24 h after the last Dox or saline injection. Brains were rapidly removed and coronal slices (300 µm) containing the PFC were cut using a Vibratome (VT1000S; Leica Microsystems) in an ice-cold artificial cerebrospinal fluid (aCSF, in mM: 130 NaCl, 3 KCl, 1.25 NaH_2PO_4, 26 $NaHCO_3$, 10 glucose, 1

JPET Fast Forward. Published on May 27, 2020 as DOI: 10.1124/jpet.120.266023
This article has not been copyedited and formatted. The final version may differ from this version.

$MgCl_2$, and 2 $CaCl_2$, pH 7.2–7.4, saturated with 95% O_2 and 5% CO_2) solution in which NaCl was replaced with an equiosmolar concentration of sucrose. Slices were incubated in aCSF at 32–34°C for 45 min and kept at 22–25°C thereafter, until transfer to the recording chamber. All solutions had osmolarity between 305 and 315 mOsm. Slices were viewed under an upright microscope (Eclipse FN1; Nikon Instruments) with infrared differential interference contrast optics and a 40 × water-immersion objective. For recordings, the chamber was continuously perfused at a rate of 1–2 mL/min with oxygenated aCSF heated to 32 ± 1°C using an automated temperature controller (Warner Instruments). Recording pipettes were pulled from borosilicate glass capillaries (World Precision Instruments) to a resistance of 4–7 MΩ when filled with the intracellular solution. The intracellular solution contained the following (in mM): 145 potassium gluconate, 2 $MgCl_2$, 2.5 KCl, 2.5 NaCl, 0.1 BAPTA, 10 HEPES, 2 Mg-ATP, and 0.5 GTP-Tris, pH 7.2–7.3, with KOH, osmolarity 280–290 mOsm. Layer V pyramidal neurons of the prelimbic cortex were identified by their morphology. The layer V pyramidal neurons of the medial prefrontal cortex were selected for two reasons: first, dopamine (D1) receptor expression is enriched in deeper layers of the prefrontal cortex (Santana and Artigas, 2017), which are primarily affected by HIV-1 Tat protein (Brailoiu et al., 2017; Kesby et al., 2017), second, the neurons projects to subcortical nuclei have been suggested to play a critical role in cognitive functioning (Douglas and Martin, 2004; Riga et al., 2014). Current step protocols (from -500 to +500 pA; 20 pA increments; 500 ms step duration) were run to determine action potential frequency versus current (*f-I*) relationship. Drugs were applied via the Y-tube perfusion system modified for optimal solution exchange in brain slices (Hevers and Luddens, 2002). Dopamine (10 nM, final concentration) was initially applied alone, followed by the combined application of dopamine (10 nM) and GBR-12909 (100 nM), followed by the combined application of dopamine (10 nM), GBR-12909 (100 nM) and desipramine (1 μM). All data were collected after a minimum of 2 min of drug exposure. Currents were low-pass filtered at 2 kHz and digitized at 20 kHz using a Digidata 1440A acquisition board (Molecular Devices) and pClamp10 software

JPET Fast Forward. Published on May 27, 2020 as DOI: 10.1124/jpet.120.266023
This article has not been copyedited and formatted. The final version may differ from this version.

(Molecular Devices). Access resistance (10–30 MΩ) was monitored during recordings by injection of 10 mV hyperpolarizing pulses. All analyses were completed using Clampfit 10 (Molecular Devices).

Data analysis

Data are expressed as mean ± S.E.M., and *n* refers to the number of individual experiments for each group. To analyze the kinetic parameters (V_{max}/K_m and B_{max}/K_d) of [^{3}H]DA uptake or [^{3}H]WIN 35,428 and [^{3}H]Nisoxetine binding, best fit non-linear regression analysis using a single site model was conducted for each individual experiment using GraphPad Prism 8 software. To determine whether a relationship existed between individual mouse age and the respective experimental data, separate Pearson correlation analysis was conducted. The kinetic parameters were then compared between the saline and Dox treated groups for C57BL/6J or G-tg mice (to rule out any non-specific effects of Dox administration) and subsequently for the iTat-tg mice using unpaired Student's *t* tests, which were conducted using IBM SPSS statistics version 25. Analyses resulting in $p < 0.05$ were considered significant.

JPET Fast Forward. Published on May 27, 2020 as DOI: 10.1124/jpet.120.266023
This article has not been copyedited and formatted. The final version may differ from this version.

Results:

Expression of HIV-1 Tat produces a decrease in synaptosomal [^{3}H]DA uptake through both DAT and NET in the PFC.

To determine the effects of Dox-induced Tat expression on DA uptake via DAT or NET, kinetic analyses of synaptosomal [^{3}H]DA uptake were performed in iTat-tg mice following 7- or 14-days of Dox administration. After 7-day administration of Dox or saline (Figure 1A and B), the V_{max} of [^{3}H]DA uptake via DAT and NET in the PFC was significantly reduced by 27 ± 4.8% [$t_{(7.953)}$ = 3.981, p < 0.01] and 27 ± 6.8% [$t_{(11)}$ = 3.752, p < 0.01], respectively, compared to the respective saline controls (Figure 1A and B). No changes in the K_m values of [^{3}H]DA uptake via DAT were observed (Figure 1A), however the K_m values of [^{3}H]DA uptake via NET of iTat Dox-treated mice were significantly reduced by 58 ± 6.6% compared to saline-treated controls [$t_{(11)}$ = 3.708, p < 0.01] (Figure 1B). After 14-day administration of Dox or saline, the V_{max} values of [^{3}H]DA uptake via DAT (Figure 1C) and NET (Figure 1D) in the PFC were significantly decreased by 30 ± 5.9% [$t_{(9)}$ = 2.356, p < 0.05] and 32 ± 3.1% [$t_{(8)}$ = 2.952, p < 0.05], respectively compared to saline-treated controls. No significant differences in the K_m of [^{3}H]DA uptake via either DAT or NET were found (Figures 1C and D). We also determined the V_{max} and K_m values of [^{3}H]DA uptake in the striatum and hippocampus where DAT and NET are dominantly expressed. Results showed no observable difference in the V_{max} and K_m values of [^{3}H]DA uptake via DAT in the striatum and NET in hippocampus between saline- and Dox-treated iTat-tg mice following either 7- or 14-day administration of Dox (Table 1). In the current study, in addition to iTat-tg mice treated with saline as a control for Dox treatment, C57BL/6J and G-tg mice were used as negative controls. No differences in the V_{max} and K_m values of [^{3}H]DA uptake via DAT and NET in those brain regions were observed between saline- or Dox-treated mice (Supplemental tables 1-3).

JPET Fast Forward. Published on May 27, 2020 as DOI: 10.1124/jpet.120.266023
This article has not been copyedited and formatted. The final version may differ from this version.

Expression of HIV-1 Tat does not alter plasmalemmal membrane expression of DAT or NET in the PFC.

To determine whether the Tat expression-induced decrease in the V_{max} of [^{3}H]DA uptake via DAT or NET in PFC was associated with an alteration of the subcellular distribution of the transporters, biotinylation and immunoblot assays were performed to assess cell surface and intracellular transporter localization. Three subcellular fractions were prepared from the PFC, striatum, and hippocampus of iTat-tg mice following 7-day Dox or saline administration and DAT or NET immunoreactivity in both total fraction and cell surface fraction (biotinylated) were examined. No differences in DAT or NET immunoreactivity in PFC between saline- and Dox-treated iTat-tg mice were found in the ratio of total or surface transporters to calnexin (Figure 2), indicating that the observed decrease in the V_{max} for DAT or NET is not due to alteration of the available transporters on the cell surface. Moreover, no differences in the respective immunoreactivity of DAT in striatum or NET in hippocampus between saline- and Dox-treated iTat-tg mice were found in the ratio of total or surface transporters to calnexin (supplemental figure 1). Additionally, no differences were observed in DAT or NET immunoreactivity in the PFC, striatum, or hippocampus between saline- and Dox-treated control mice in the ratio of total or surface transporters to calnexin (Supplemental figure 2).

Expression of HIV-1 Tat produces a decrease in [^{3}H]WIN 35,428 and [^{3}H]Nisoxetine binding in the PFC

[^{3}H]WIN 35,428 and [^{3}H]Nisoxetine are highly selective and potent reuptake inhibitors with high affinity for the DAT and NET, respectively (Tejani-Butt, 1992; Pristupa et al., 1994). To determine whether Tat-induced decreases in the V_{max} of [^{3}H]DA uptake via DAT or NET alter the respective substrate binding sites, kinetic analyses of [^{3}H]WIN 35,428 and [^{3}H]Nisoxetine binding were performed in the brain regions of iTat-tg mice following 7-day Dox or saline administration. For [^{3}H]WIN 35,428 binding sites, in comparison to saline controls, the B_{max}

JPET Fast Forward. Published on May 27, 2020 as DOI: 10.1124/jpet.120.266023
This article has not been copyedited and formatted. The final version may differ from this version.

values in PFC of Dox-treated iTat-tg mice were decreased by 28 ± 2.7% [$t_{(7)}$ = 4.396, $p < 0.01$] (Figure 3A), with no change in K_d values. However, no difference was observed in the B_{max} values in striatum between saline-and Dox-treated iTat-tg mice (Table 1). For [^{3}H]Nisoxetine binding sites, the B_{max} values in the PFC of Dox-treated iTat-tg mice was reduced by 36 ± 7.7% compared to saline-treated controls [$t_{(7)}$ = 2.479, $p < 0.05$] (Figure 3B). The K_d value was reduced by 40 ± 10% compared to saline-treated controls [$t_{(8)}$ = 2.670, $p < 0.05$] (Figure 3B). No difference in the B_{max} values in hippocampus were found between saline-and Dox-treated iTat-tg mice (Table 1). Moreover, no differences were observed between saline- or Dox-treated control mice (supplemental tables 1 and 2).

Due to the comparable decreases observed in the V_{max} of [^{3}H]DA uptake and the B_{max} of [^{3}H]WIN 35,428 binding for the DAT in the PFC of Dox-treated iTat mice, comparison of the turnover rate (V_{max}/B_{max}) revealed no significant differences between saline (2.43 ± 0.14) and Dox (2.16 ± 0.29) treated groups (Figure 3C). Analysis of the ratio of K_m and K_d for V_{max} of [^{3}H]DA uptake and the B_{max} of [^{3}H]WIN 35,428 binding for the DAT in the PFC also revealed no significant differences between saline (0.014 ± 0.005) and Dox (0.009 ± 0.001) treated mice (Figure 3D). No significant differences were found in turnover rate for [^{3}H]DA uptake and [^{3}H]Nisoxetine binding for the NET in the PFC between saline (3.40 ± 0.38) and Dox (3.66 ± 0.19) treated mice (Figure 3E), or for the ratio K_m and K_d in the saline (0.013 ± 0.003) and Dox (0.011 ± 0.001) treated groups (Figure 3F).

The decreased DAT and NET function in the PFC is consistent with alterations in DA and DOPAC tissue content

Given the critical role of the DAT and the NET in controlling DA homeostasis, a Tat-induced decrease in DA reuptake via DAT or NET in the PFC could result in alterations in the levels of DA and its primary metabolite DOPAC in the respective brain regions. DA and DOPAC content were determined in PFC and striatum from iTat-tg and G-tg mice following 7-day

JPET Fast Forward. Published on May 27, 2020 as DOI: 10.1124/jpet.120.266023
This article has not been copyedited and formatted. The final version may differ from this version.

administration of saline or Dox. As shown in Figure 4, DA tissue content in PFC from Dox-treated iTat-tg mice was increased by 268% (0.078 ± 0.021 ng/mg tissue) compared to saline (0.021 ± 0.011 ng/mg tissue) treated controls [$t_{(8)} = 2.39$, $p < 0.05$] (Figure 4A). Similarly, DOPAC tissue content in the PFC of Dox-treated iTat-tg mice was increased by 144% (0.036 ± 0.006 ng/mg tissue) compared to saline (0.015 ± 0.003 ng/mg tissue) treated controls [$t_{(7)} = 3.344$, $p < 0.05$] (Figure 4B). However, neither DA or DOPAC content in striatum of iTat-tg mice differed significantly between saline- and Dox-treated groups (Figure 4C and D). We also examined the tissue levels of DA and DOPAC content in the PFC and striatum of G-tg mice, which showed no significant differences between saline- and Dox-treated groups (Supplemental Figure 3).

Action potential frequency is decreased in layer V pyramidal neurons of the prelimbic cortex of iTat-tg mice

To determine whether the Tat-induced decrease in DA uptake via DAT/NET in the PFC alters electrical firing signaling of neurons in this region, we performed whole-cell patch clamp electrophysiology on layer V pyramidal neurons in the prelimbic region of PFC from iTat-tg mice following 7-day saline or Dox treatment. As shown in Figure 5B, ANOVA analysis revealed a significant main effect of current injection [$F_{(10, 210)} = 82.52$, $p < 0.0001$], and a significant main effect of drug treatment (saline vs dox) [$F_{(1, 21)} = 5.77$, $p = 0.025$], as well as significant current × drug treatment interaction [$F_{(10, 210)} = 2.49$, $p = 0.008$]. Dox-treated iTat-tg mice displayed a reduction of action potential output in this subset of neurons, compared to saline control group (Bonferroni $p < 0.05$). No differences were observed between saline and Dox treated C57BL/6J mice (Supplemental figure 4).

Additionally, to assess the effects of inhibition of DAT or NET in the prelimbic region of PFC by selective inhibitors for the respective transporter on the observed decrease in action potential output, the basal action potentials from pyramidal neurons of iTat-tg mice with Dox or

JPET Fast Forward. Published on May 27, 2020 as DOI: 10.1124/jpet.120.266023
This article has not been copyedited and formatted. The final version may differ from this version.

saline treatment were subsequently examined in the presence of DA (10 nM), DA + GBR-12909 (a potent DAT inhibitor; 100 nM), and DA + GBR-12909 + desipramine (DMI; a potent NET inhibitor, 1 μM). A two-way ANOVA with repeated measurement on action potential in iTat-tg mice treated with saline (Figure 5C) and Dox (Figure 5D) revealed a significant main effect of current injection [saline: $F_{(10, 80)} = 21.17$, $p < 0.0001$; Dox: $F_{(10, 40)} = 145.4$, $p < 0.0001$]; however, neither saline- or Dox-treated mice displayed a significant main effect of drug exposure [saline: $F_{(3, 24)} = 1.005$, $p = 0.4$; Dox: $F_{(3, 12)} = 1.945$, $p = 0.18$]. Although the current injection × drug exposure interaction was not significant in saline-treated mice [$F_{(30, 240)} = 0.788$, $p = 0.78$], Dox-treated mice displayed a significant interaction between current injection × drug exposure [$F_{(30, 120)} = 1.571$, $p = 0.05$].

JPET Fast Forward. Published on May 27, 2020 as DOI: 10.1124/jpet.120.266023
This article has not been copyedited and formatted. The final version may differ from this version.

Discussion

The current study investigated the mechanism by which inducible Tat expression influences dopaminergic transmission in the PFC of iTat-tg mice. We have demonstrated that *in vitro* HIV-1 recombinant Tat_{1-86} protein reduces [^{3}H]DA uptake though DAT in cells (Midde et al., 2013; Midde et al., 2015; Quizon et al., 2016; Sun et al., 2017) and rat striatal synaptosomes (Zhu et al., 2009b). Our current results show that the V_{max} of [^{3}H]DA uptake through both DAT and NET was decreased in the PFC of iTat-tg mice following 7- or 14-day Dox-induced Tat_{1-86} expression. We also observed corresponding decreases in the B_{max} of [^{3}H]WIN35,428 and [^{3}H]Nisoxitine binding in this region, suggesting that the inhibitory effects of *in vitro* Tat on DAT and NET function can be replicated in the PFC of the iTat-tg mouse model with *in vivo* biological Tat expression. Moreover, we also observed increased DA and DOPAC tissue content in the iTat-tg mice, which was again selective to the PFC, suggesting a neuroadaptive change in the DA system, perhaps in compensation for iTat protein-induced inhibition of DAT and NET function.

The most intriguing observation is that the V_{max} for DA uptake via DAT or NET in the PFC was decreased (~30%) in iTat-tg mice following 7- or 14-day administration of Dox, whereas no differences in V_{max} were observed in the striatum or hippocampus of the iTat-tg mice between saline- and Dox-treated subjects. In addition, no differences in V_{max} were found in these brain regions between saline- and Dox-treated subjects in the control G-tg and C57BL/6J mouse lines. These findings suggest that the Dox-induced Tat reduces DA transport in the PFC by inhibiting both DAT and NET in a region-specific manner. Moreover, following 7-day Dox treatment, the B_{max} value for [^{3}H]WIN 35,428 labeled DAT binding sites in the PFC was decreased by 28% in iTat-tg mice, which is comparable to the magnitude of the decrease in V_{max} for DAT, whereas the B_{max} value for [^{3}H]Nisoxetine labeled NET binding sites in the PFC was decreased by 35%, which was slightly more than the observed decrease in the V_{max} for

JPET Fast Forward. Published on May 27, 2020 as DOI: 10.1124/jpet.120.266023
This article has not been copyedited and formatted. The final version may differ from this version.

NET. Interestingly, DA uptake turnover (V_{max}/B_{max}), the efficacy of DA molecules being transported per second per uptake site (Lin et al., 2000), was not altered in the PFC of iTat-tg mice, which is consistent with our previous results showing no change in DA uptake turnover following *in vitro* exposure of rat synaptosomes to Tat (Midde et al., 2012). The efficacy of DA uptake largely depends on DAT expression in the plasma membrane, which is dynamically modulated by a trafficking mechanism (Zhu and Reith, 2008). Results from the surface biotinylation assay did not find any difference in total and plasma membrane expression of DAT or NET in the PFC in iTat-tg mice between Dox- and saline-treated groups, suggesting that the reductions in V_{max} and B_{max} are not due to Tat-induced transporter protein degradation or surface transporter trafficking. We have demonstrated that DA transport to cytoplasmic pool via DAT is a dynamic conversion of the transporter‘s conformation between the three states (outward-open, outward-occluded, and inward-open) (Yuan et al., 2016) and that the Tat protein allosterically regulates DAT activity by binding to DAT in the outward-open state (Yuan et al., 2015; Zhu et al., 2018). Considering that DAT and NET share similar binding residues for Tat based on computational and homology modeling (Yuan et al., 2016), the Dox-induced Tat expression could reduce both V_{max} and B_{max} for DAT/NET by interfering with the Tat-DAT/NET binding sites and inducing a conformational change of DAT/NET from the outward-open state to the outward-occluded state.

The equivariant expression of inducible Tat protein across all brain regions in the iTat-tg mice subjected to 7 days of 100 mg/kg/day Dox treatment has been confirmed by detecting Tat mRNA (Kim et al., 2003) and Tat immunoblotting (Carey et al., 2012). A caveat, however, it is unclear what is the actual concentration of Dox-induced Tat expression is at or around the synaptic terminals, and how this effective concentration of Tat might be reflected in the brain of HIV-infected patients remains unclear, as most studies investigating the inhibitory effects of Tat on monoamine transporters are performed *in vitro* using recombinant Tat. For example,

JPET Fast Forward. Published on May 27, 2020 as DOI: 10.1124/jpet.120.266023
This article has not been copyedited and formatted. The final version may differ from this version.

exposure to 140 nM recombinant Tat_{1-86} induces about 30% reduction of DA uptake in cells expressing wild-type hDAT (Midde et al., 2013; Midde et al., 2015; Quizon et al., 2016; Sun et al., 2017) and brain synaptosomes (Zhu et al., 2009b). One study reported that a detectable Tat concentration in frontal cortical brain samples from HIV-1-infected patients is about 140 pmol (Hudson et al., 2000), which is 1000-fold lower than *in vitro* recombinant Tat used in reported studies. The Dox treatment of 100 mg/kg used in this study has been shown to induce ~ 1 ng/mL Tat concentration in the iTat-tg mouse brain (Kim et al., 2003), which is comparable to Tat protein levels detected in sera of HIV+ patients (Westendorp et al., 1995; Xiao et al., 2000). Nevertheless, our studies with *in vitro* and *in vivo* Tat exposure provide molecular insight into the mechanisms underlying Tat-induced dysregulation of dopaminergic transmission via DAT and NET.

Consistent with the decreased V_{max} for DAT and NET in PFC, the current study found an increase in the tissue content of DA and DOPAC in the PFC of iTat-tg mice 24 h after 7-day administration of Dox. Similar studies have demonstrated increased DA content in the caudate putamen of iTat-tg mice 3 days after completing a 7-day Dox regiment (Kesby et al., 2016a), but decreased ratios of DOPAC/DA in the same region 10 days after completing a 7-day Dox regiment without changes in this ratio in PFC (Kesby et al., 2016b). Regarding these results, effects of Tat on DA tissue content in specific brain regions may be influenced by different Dox regiments and the timing of brain collection after Dox treatment. Levels of extracellular DA in the synaptic cleft are controlled by reuptake via plasma membrane transporters and presynaptic vesicle-mediated release. Indeed, we have demonstrated that *in vitro* exposure to Tat inhibits DA uptake via the vesicular monoamine transporter-2 (Midde et al., 2012), which is responsible for monoamine storage and the vesicle-mediated DA release. Therefore, a very complex influence of Tat protein on the DA system should be taken into consideration when we evaluate the actual DA levels in iTat-tg mice after Dox-induced Tat expression. Given that the DA content

JPET Fast Forward. Published on May 27, 2020 as DOI: 10.1124/jpet.120.266023
This article has not been copyedited and formatted. The final version may differ from this version.

reflects the tissue levels of total DA rather than the specific extracellular DA levels, monitoring release and uptake dynamics of endogenous DA levels in iTat-tg mice by an electrochemical technique (e.g. fast scan cyclic voltammetry) is an interesting topic for future investigation.

Another important finding from the current study is that the inhibitory effects of Tat on the kinetic parameters of DA uptake through DAT/NET and the respective substrate binding sites are selective to the PFC. There are several possible explanations for our observations. First, compared to the PFC, the striatum and hippocampus exhibit a higher density of DAT and NET (Horn, 1973b; Raiteri et al., 1977; Borgkvist et al., 2012), which may provide protection from the acute inhibitory effects of HIV-1 Tat on transporter function. Second, HIV-1 Tat may be not expressed equally throughout different brain regions. Although a previous report showed Tat immunoreactivity was expressed throughout brain of the Tat transgenic mice (Carey et al., 2012), the exact concentration of biological Tat in these brain regions remains unclear. Indeed, our previous study has reported that HIV-1 Tat inhibits DAT function in a concentration-dependent manner (Zhu et al., 2009b). Third, with regards to HIV-1 Tat-induced decrease in DA transport through NET, the NET in the PFC is more concentrated than the DAT and plays a primary role in reuptake of DA (Moll et al., 2000; Moron et al., 2002). For these reasons, it is possible that HIV-1 Tat-induced dysfunction of the DA system in the PFC could be mediated by inhibition of both DAT and NET. In the early stages of HIV-1 infection, the cognitive impairments associated with the PFC is initially observed (Everall et al., 1991; Melrose et al., 2008), whereas the severe damage such as degradation of the dopaminergic terminals is observed in the striatal area in the late stages of HIV-1 infected patients (Wang et al., 2004; Chang et al., 2008). Moreover, volume loss and thinning of the PFC are found in the patients with AIDS, which is associated with the severity of cognitive impairments (Thompson et al., 2005), suggesting that the PFC is more vulnerable to HIV infection compared to other regions. Thus, the current

JPET Fast Forward. Published on May 27, 2020 as DOI: 10.1124/jpet.120.266023
This article has not been copyedited and formatted. The final version may differ from this version.

findings demonstrate that the inhibition of DAT/NET specifically in the PFC may play an important role in mediating Tat-induced neurocognitive impairment observed in HAND.

Whole-cell patch clamp recordings show that the evoked basal action potential firing from layer V pyramidal neurons of the prelimbic cortex is reduced in iTat-tg mice treated with Dox compared to saline controls. This reduced neuronal firing is unlikely to have resulted from the Tat-induced decrease in DA uptake via DAT and NET since DA at the low concentration used in our experiments has no effect on action potentials and previous studies indicate that higher concentrations of DA increase membrane excitability in striatal as well as prefrontocortical projection neurons (Hopf et al., 2003; Ortinski et al., 2015; Buchta et al., 2017; Lahiri and Bevan, 2020). Conversely, reduced neuronal firing is unlikely to have caused a deficit in DAT function via effects on membrane potential, since membrane hypoexcitability has been linked to surface expression of DAT (Richardson et al., 2016). Finally, DAT-mediated translocation of Na^+ ions across the plasma membrane is not expected to have a pronounced impact on either the membrane potential or spike firing and a trend towards reduced action potential firing with desipramine of AMPA-mediated currents and voltage-gated Ca^{2+} channels (Koncz et al., 2014). Together, these observations suggest that decreased action potential firing of prelimbic cortex pyramidal neurons in iTat-tg mice is not directly related to Tat effects on DA transport. HIV-1 Tat may, however, affect action potential generation through mechanisms independent of DA uptake with a variety of bi-directional effects reported by previous studies (Krogh et al., 2014; Ngwainmbi et al., 2014; Francesconi et al., 2018; Mohseni Ahooyi et al., 2018).

In conclusion, the current findings provide a novel evidence that HIV-1 Tat protein decreases the V_{max} pf [^{3}H]DA uptake and the respective substrate binding sites in the PFC of iTat-tg mice by inhibiting both DAT and NET, which may have important implications for

JPET Fast Forward. Published on May 27, 2020 as DOI: 10.1124/jpet.120.266023
This article has not been copyedited and formatted. The final version may differ from this version.

preclinical studies if the role of the prefrontal DAT/NET in neurocognitive impairment observed in HAND. Considering HIV-1 Tat interacting with allosteric modulatory binding sites on these transporters (Zhu et al., 2011; Sun et al., 2017), the current study provides a biological basis for developing allosteric modulators that specifically block Tat binding on these transporters with minimal effect on physiological DA transport, which may have potential for therapeutic application in Tat-induced dysregulation of dopaminergic transmission and its associated cognitive deficits observed in HIV-1 infected patients.

Acknowledgments:

We thank Wei-Lun Sun and Luyi Zhou for technical assistance.

JPET Fast Forward. Published on May 27, 2020 as DOI: 10.1124/jpet.120.266023
This article has not been copyedited and formatted. The final version may differ from this version.

Authorship Contributions:

Participated in research design: Strauss, Ortinski, Zhu

Conducted experiments: Strauss, O'Donovan, Ma, Xiao, Lin, Bardo

Contributed animals and provided guidance of Tat induction procedures: McLaughlin

Performed data analysis: Strauss, Bardo, O'Donovan, Zhu

Wrote or contributed to the writing and editing of the manuscript: Strauss, O'Donovan, Zhu

JPET Fast Forward. Published on May 27, 2020 as DOI: 10.1124/jpet.120.266023
This article has not been copyedited and formatted. The final version may differ from this version.

References

Berger JR and Arendt G (2000) HIV dementia: the role of the basal ganglia and dopaminergic systems. *Journal of psychopharmacology* **14**:214-221.

Borgkvist A, Malmlof T, Feltmann K, Lindskog M and Schilstrom B (2012) Dopamine in the hippocampus is cleared by the norepinephrine transporter. *Int J Neuropsychopharmacol* **15**:531-540.

Brack-Werner R (1999) Astrocytes: HIV cellular reservoirs and important participants in neuropathogenesis. *AIDS* **13**:1-22.

Bradford MM (1976) A rapid and sensitive method for the quantitation of microgram quantities of protein utilizing the principle of protein-dye binding. *Anal Biochem* **72**:248-254.

Brailoiu GC, Deliu E, Barr JL, Console-Bram LM, Ciuciu AM, Abood ME, Unterwald EM and Brailoiu E (2017) HIV Tat excites D1 receptor-like expressing neurons from rat nucleus accumbens. *Drug Alcohol Depend* **178**:7-14.

Buchta WC, Mahler SV, Harlan B, Aston-Jones GS and Riegel AC (2017) Dopamine terminals from the ventral tegmental area gate intrinsic inhibition in the prefrontal cortex. *Physiol Rep* **5**.

Buckner CM, Luers AJ, Calderon TM, Eugenin EA and Berman JW (2006) Neuroimmunity and the blood-brain barrier: molecular regulation of leukocyte transmigration and viral entry into the nervous system with a focus on neuroAIDS. *J Neuroimmune Pharmacol* **1**:160-181.

Carey AN, Liu X, Mintzopoulos D, Paris JJ, Muschamp JW, McLaughlin JP and Kaufman MJ (2013) Conditional Tat protein expression in the GT-tg bigenic mouse brain induces gray matter density reductions. *Prog Neuropsychopharmacol Biol Psychiatry* **43**:49-54.

Carey AN, Sypek EI, Singh HD, Kaufman MJ and McLaughlin JP (2012) Expression of HIV-Tat protein is associated with learning and memory deficits in the mouse. *Behav Brain Res* **229**:48-56.

Chang L, Wang GJ, Volkow ND, Ernst T, Telang F, Logan J and Fowler JS (2008) Decreased brain dopamine transporters are related to cognitive deficits in HIV patients with or without cocaine abuse. *Neuroimage* **42**:869-878.

Cools R (2006) Dopaminergic modulation of cognitive function-implications for L-DOPA treatment in Parkinson's disease. *Neurosci Biobehav Rev* **30**:1-23.

Dalley JW, Cardinal RN and Robbins TW (2004) Prefrontal executive and cognitive functions in rodents: neural and neurochemical substrates. *Neurosci Biobehav Rev* **28**:771-784.

Del Valle L, Croul S, Morgello S, Amini S, Rappaport J and Khalili K (2000) Detection of HIV-1 Tat and JCV capsid protein, VP1, in AIDS brain with progressive multifocal leukoencephalopathy. *J Neurovirol* **6**:221-228.

Douglas RJ and Martin KA (2004) Neuronal circuits of the neocortex. *Annu Rev Neurosci* **27**:419-451.

Everall IP, Luthert PJ and Lantos PL (1991) Neuronal loss in the frontal cortex in HIV infection. *Lancet* **337**:1119-1121.

Francesconi W, Berton F and Marcondes MCG (2018) HIV-1 Tat alters neuronal intrinsic excitability. *BMC Res Notes* **11**:275.

Frankel AD and Young JA (1998) HIV-1: fifteen proteins and an RNA. *Annu Rev Biochem* **67**:1-25.

Gaskill PJ, Calderon TM, Luers AJ, Eugenin EA, Javitch JA and Berman JW (2009) Human immunodeficiency virus (HIV) infection of human macrophages is increased by dopamine: a bridge between HIV-associated neurologic disorders and drug abuse. *Am J Pathol* **175**:1148-1159.

Gelman BB, Lisinicchia JG, Chen T, Johnson KM, Jennings K, Freeman DH, Jr. and Soukup VM (2012) Prefrontal Dopaminergic and Enkephalinergic Synaptic Accommodation in

HIV-associated Neurocognitive Disorders and Encephalitis. *J Neuroimmune Pharmacol* **7**:686-700.

Heaton RK, Clifford DB, Franklin DR, Jr., Woods SP, Ake C, Vaida F, Ellis RJ, Letendre SL, Marcotte TD, Atkinson JH, Rivera-Mindt M, Vigil OR, Taylor MJ, Collier AC, Marra CM, Gelman BB, McArthur JC, Morgello S, Simpson DM, McCutchan JA, Abramson I, Gamst A, Fennema-Notestine C, Jernigan TL, Wong J, Grant I and Group C (2010) HIV-associated neurocognitive disorders persist in the era of potent antiretroviral therapy: CHARTER Study. *Neurology* **75**:2087-2096.

Henderson LJ, Johnson TP, Smith BR, Reoma LB, Santamaria UA, Bachani M, Demarino C, Barclay RA, Snow J, Sacktor N, McArthur J, Letendre S, Steiner J, Kashanchi F and Nath A (2019) Presence of Tat and transactivation response element in spinal fluid despite antiretroviral therapy. *AIDS* **33 Suppl 2**:S145-S157.

Hevers W and Luddens H (2002) Pharmacological heterogeneity of gamma-aminobutyric acid receptors during development suggests distinct classes of rat cerebellar granule cells in situ. *Neuropharmacology* **42**:34-47.

Hopf FW, Cascini MG, Gordon AS, Diamond I and Bonci A (2003) Cooperative activation of dopamine D1 and D2 receptors increases spike firing of nucleus accumbens neurons via G-protein betagamma subunits. *J Neurosci* **23**:5079-5087.

Horn AS (1973a) Structure-activity relations for the inhibition of catecholamine uptake into synaptosomes from noradrenaline and dopaminergic neurones in rat brain homogenates. *Br J Pharmacol* **47**:332-338.

Horn AS (1973b) Structure activity relations for the inhibition of 5-HT uptake into rat hypothalamic homogenates by serotonin and tryptamine analogues. *J Neurochem* **21**:883-888.

Hudson L, Liu J, Nath A, Jones M, Raghavan R, Narayan O, Male D and Everall I (2000) Detection of the human immunodeficiency virus regulatory protein tat in CNS tissues. *J Neurovirol* **6**:145-155.

Johnson TP, Patel K, Johnson KR, Maric D, Calabresi PA, Hasbun R and Nath A (2013) Induction of IL-17 and nonclassical T-cell activation by HIV-Tat protein. *Proc Natl Acad Sci U S A* **110**:13588-13593.

Johnston JB, Zhang K, Silva C, Shalinsky DR, Conant K, Ni W, Corbett D, Yong VW and Power C (2001) HIV-1 Tat neurotoxicity is prevented by matrix metalloproteinase inhibitors. *Ann Neurol* **49**:230-241.

Kesby JP, Markou A and Semenova S (2016a) The effects of HIV-1 regulatory TAT protein expression on brain reward function, response to psychostimulants and delay-dependent memory in mice. *Neuropharmacology* **109**:205-215.

Kesby JP, Markou A, Semenova S and Group T (2016b) Effects of HIV/TAT protein expression and chronic selegiline treatment on spatial memory, reversal learning and neurotransmitter levels in mice. *Behav Brain Res* **311**:131-140.

Kesby JP, Najera JA, Romoli B, Fang Y, Basova L, Birmingham A, Marcondes MCG, Dulcis D and Semenova S (2017) HIV-1 TAT protein enhances sensitization to methamphetamine by affecting dopaminergic function. *Brain, behavior, and immunity* **65**:210-221.

Kim BO, Liu Y, Ruan Y, Xu ZC, Schantz L and He JJ (2003) Neuropathologies in transgenic mice expressing human immunodeficiency virus type 1 Tat protein under the regulation of the astrocyte-specific glial fibrillary acidic protein promoter and doxycycline. *Am J Pathol* **162**:1693-1707.

King JE, Eugenin EA, Buckner CM and Berman JW (2006) HIV tat and neurotoxicity. *Microbes and infection / Institut Pasteur* **8**:1347-1357.

Koncz I, Szasz BK, Szabo SI, Kiss JP, Mike A, Lendvai B, Sylvester Vizi E and Zelles T (2014) The tricyclic antidepressant desipramine inhibited the neurotoxic, kainate-induced

[Ca(2+)]i increases in CA1 pyramidal cells in acute hippocampal slices. *Brain Res Bull* **104**:42-51.

Koutsilieri E, Sopper S, Scheller C, ter Meulen V and Riederer P (2002) Involvement of dopamine in the progression of AIDS Dementia Complex. *J Neural Transm (Vienna)* **109**:399-410.

Krogh KA, Green MV and Thayer SA (2014) HIV-1 Tat-induced changes in synaptically-driven network activity adapt during prolonged exposure. *Curr HIV Res* **12**:406-414.

Kumar AM, Fernandez JB, Singer EJ, Commins D, Waldrop-Valverde D, Ownby RL and Kumar M (2009) Human immunodeficiency virus type 1 in the central nervous system leads to decreased dopamine in different regions of postmortem human brains. *J Neurovirol* **15**:257-274.

Kumar AM, Ownby RL, Waldrop-Valverde D, Fernandez B and Kumar M (2011) Human immunodeficiency virus infection in the CNS and decreased dopamine availability: relationship with neuropsychological performance. *J Neurovirol* **17**:26-40.

Lahiri AK and Bevan MD (2020) Dopaminergic Transmission Rapidly and Persistently Enhances Excitability of D1 Receptor-Expressing Striatal Projection Neurons. *Neuron*.

Lamers SL, Salemi M, Galligan DC, Morris A, Gray R, Fogel G, Zhao L and McGrath MS (2010) Human immunodeficiency virus-1 evolutionary patterns associated with pathogenic processes in the brain. *J Neurovirol* **16**:230-241.

Lammel S, Lim BK, Ran C, Huang KW, Betley MJ, Tye KM, Deisseroth K and Malenka RC (2012) Input-specific control of reward and aversion in the ventral tegmental area. *Nature* **491**:212-217.

Lin Z, Itokawa M and Uhl GR (2000) Dopamine transporter proline mutations influence dopamine uptake, cocaine analog recognition, and expression. *FASEB J* **14**:715-728.

Meade CS, Lowen SB, MacLean RR, Key MD and Lukas SE (2011) fMRI brain activation during a delay discounting task in HIV-positive adults with and without cocaine dependence. *Psychiatry Res* **192**:167-175.

Melrose RJ, Tinaz S, Castelo JM, Courtney MG and Stern CE (2008) Compromised fronto-striatal functioning in HIV: an fMRI investigation of semantic event sequencing. *Behav Brain Res* **188**:337-347.

Midde NM, Gomez AM and Zhu J (2012) HIV-1 Tat protein decreases dopamine transporter cell surface expression and vesicular monoamine transporter-2 function in rat striatal synaptosomes. *J Neuroimmune Pharmacol* **7**:629-639.

Midde NM, Huang X, Gomez AM, Booze RM, Zhan CG and Zhu J (2013) Mutation of tyrosine 470 of human dopamine transporter is critical for HIV-1 Tat-induced inhibition of dopamine transport and transporter conformational transitions. *J Neuroimmune Pharmacol* **8**:975-987.

Midde NM, Yuan Y, Quizon PM, Sun WL, Huang X, Zhan CG and Zhu J (2015) Mutations at tyrosine 88, lysine 92 and tyrosine 470 of human dopamine transporter result in an attenuation of HIV-1 Tat-induced inhibition of dopamine transport. *J Neuroimmune Pharmacol* **10**:122-135.

Miller EK and Cohen JD (2001) An integrative theory of prefrontal cortex function. *Annu Rev Neurosci* **24**:167-202.

Mohseni Ahooyi T, Shekarabi M, Decoppet EA, Langford D, Khalili K and Gordon J (2018) Network analysis of hippocampal neurons by microelectrode array in the presence of HIV-1 Tat and cocaine. *J Cell Physiol* **233**:9299-9311.

Moll GH, Mehnert C, Wicker M, Bock N, Rothenberger A, Ruther E and Huether G (2000) Age-associated changes in the densities of presynaptic monoamine transporters in different regions of the rat brain from early juvenile life to late adulthood. *Brain Res Dev Brain Res* **119**:251-257.

Moron JA, Brockington A, Wise RA, Rocha BA and Hope BT (2002) Dopamine uptake through the norepinephrine transporter in brain regions with low levels of the dopamine transporter: evidence from knock-out mouse lines. *J Neurosci* **22**:389-395.

Nath A, Jankovic J and Pettigrew LC (1987) Movement disorders and AIDS. *Neurology* **37**:37-41.

Ngwainmbi J, De DD, Smith TH, El-Hage N, Fitting S, Kang M, Dewey WL, Hauser KF and Akbarali HI (2014) Effects of HIV-1 Tat on enteric neuropathogenesis. *J Neurosci* **34**:14243-14251.

Nieoullon A (2002) Dopamine and the regulation of cognition and attention. *Prog Neurobiol* **67**:53-83.

Ortinski PI, Briand LA, Pierce RC and Schmidt HD (2015) Cocaine-seeking is associated with PKC-dependent reduction of excitatory signaling in accumbens shell D2 dopamine receptor-expressing neurons. *Neuropharmacology* **92**:80-89.

Paris JJ, Fenwick J and McLaughlin JP (2014a) Estrous cycle and HIV-1 Tat protein influence cocaine-conditioned place preference and induced locomotion of female mice. *Curr HIV Res* **12**:388-396.

Paris JJ, Singh HD, Ganno ML, Jackson P and McLaughlin JP (2014b) Anxiety-like behavior of mice produced by conditional central expression of the HIV-1 regulatory protein, Tat. *Psychopharmacology (Berl)* **231**:2349-2360.

Power C, McArthur JC, Nath A, Wehrly K, Mayne M, Nishio J, Langelier T, Johnson RT and Chesebro B (1998) Neuronal death induced by brain-derived human immunodeficiency virus type 1 envelope genes differs between demented and nondemented AIDS patients. *J Virol* **72**:9045-9053.

Pristupa ZB, Wilson JM, Hoffman BJ, Kish SJ and Niznik HB (1994) Pharmacological heterogeneity of the cloned and native human dopamine transporter: disassociation of [3H]WIN 35,428 and [3H]GBR 12,935 binding. *Mol Pharmacol* **45**:125-135.

Purohit V, Rapaka R and Shurtleff D (2011) Drugs of abuse, dopamine, and HIV-associated neurocognitive disorders/HIV-associated dementia. *Molecular neurobiology* **44**:102-110.

Quizon PM, Sun WL, Yuan Y, Midde NM, Zhan CG and Zhu J (2016) Molecular mechanism: the human dopamine transporter histidine 547 regulates basal and HIV-1 Tat protein-inhibited dopamine transport. *Scientific reports* **6**:39048.

Raiteri M, Del Carmine R, Bertollini A and Levi G (1977) Effect of sympathomimetic amines on the synaptosomal transport of noradrenaline, dopamine and 5-hydroxytryptamine. *Eur J Pharmacol* **41**:133-143.

Rappaport J, Joseph J, Croul S, Alexander G, Del Valle L, Amini S and Khalili K (1999) Molecular pathway involved in HIV-1-induced CNS pathology: role of viral regulatory protein, Tat. *Journal of leukocyte biology* **65**:458-465.

Reith ME, Wang LC and Dutta AK (2005) Pharmacological profile of radioligand binding to the norepinephrine transporter: instances of poor indication of functional activity. *J Neurosci Methods* **143**:87-94.

Richardson BD, Saha K, Krout D, Cabrera E, Felts B, Henry LK, Swant J, Zou MF, Newman AH and Khoshbouei H (2016) Membrane potential shapes regulation of dopamine transporter trafficking at the plasma membrane. *Nature communications* **7**:10423.

Ridderinkhof KR, van den Wildenberg WP, Segalowitz SJ and Carter CS (2004) Neurocognitive mechanisms of cognitive control: the role of prefrontal cortex in action selection, response inhibition, performance monitoring, and reward-based learning. *Brain and cognition* **56**:129-140.

Riga D, Matos MR, Glas A, Smit AB, Spijker S and Van den Oever MC (2014) Optogenetic dissection of medial prefrontal cortex circuitry. *Front Syst Neurosci* **8**:230.

Santana N and Artigas F (2017) Laminar and Cellular Distribution of Monoamine Receptors in Rat Medial Prefrontal Cortex. *Front Neuroanat* **11**:87.

Sardar AM, Czudek C and Reynolds GP (1996) Dopamine deficits in the brain: the neurochemical basis of parkinsonian symptoms in AIDS. *Neuroreport* **7**:910-912.

Scheller C, Arendt G, Nolting T, Antke C, Sopper S, Maschke M, Obermann M, Angerer A, Husstedt IW, Meisner F, Neuen-Jacob E, Muller HW, Carey P, Ter Meulen V, Riederer P and Koutsilieri E (2010) Increased dopaminergic neurotransmission in therapy-naive asymptomatic HIV patients is not associated with adaptive changes at the dopaminergic synapses. *J Neural Transm* **117**:699-705.

Sun WL, Quizon PM, Yuan Y, Zhang W, Ananthan S, Zhan CG and Zhu J (2017) Allosteric modulatory effects of SRI-20041 and SRI-30827 on cocaine and HIV-1 Tat protein binding to human dopamine transporter. *Scientific reports* **7**:3694.

Tejani-Butt SM (1992) [3H]nisoxetine: a radioligand for quantitation of norepinephrine uptake sites by autoradiography or by homogenate binding. *Journal of Pharmacology and Experimental Therapeutics* **260**:427-436.

Thompson PM, Dutton RA, Hayashi KM, Toga AW, Lopez OL, Aizenstein HJ and Becker JT (2005) Thinning of the cerebral cortex visualized in HIV/AIDS reflects CD4+ T lymphocyte decline. *Proc Natl Acad Sci U S A* **102**:15647-15652.

Tye KM, Mirzabekov JJ, Warden MR, Ferenczi EA, Tsai HC, Finkelstein J, Kim SY, Adhikari A, Thompson KR, Andalman AS, Gunaydin LA, Witten IB and Deisseroth K (2013) Dopamine neurons modulate neural encoding and expression of depression-related behaviour. *Nature* **493**:537-541.

Wang GJ, Chang L, Volkow ND, Telang F, Logan J, Ernst T and Fowler JS (2004) Decreased brain dopaminergic transporters in HIV-associated dementia patients. *Brain* **127**:2452-2458.

Westendorp MO, Frank R, Ochsenbauer C, Stricker K, Dhein J, Walczak H, Debatin KM and Krammer PH (1995) Sensitization of T cells to CD95-mediated apoptosis by HIV-1 Tat and gp120. *Nature* **375**:497-500.

Williams JM and Steketee JD (2004) Characterization of dopamine transport in crude synaptosomes prepared from rat medial prefrontal cortex. *J Neurosci Methods* **137**:161-165.

Xiao H, Neuveut C, Tiffany HL, Benkirane M, Rich EA, Murphy PM and Jeang KT (2000) Selective CXCR4 antagonism by Tat: implications for in vivo expansion of coreceptor use by HIV-1. *Proc Natl Acad Sci U S A* **97**:11466-11471.

Yuan Y, Huang X, Midde NM, Quizon PM, Sun WL, Zhu J and Zhan CG (2015) Molecular mechanism of HIV-1 Tat interacting with human dopamine transporter. *ACS chemical neuroscience* **6**:658-665.

Yuan Y, Huang X, Zhu J and Zhan CG (2016) Computational modeling of human dopamine transporter structures, mechanism and its interaction with HIV-1 transactivator of transcription. *Future medicinal chemistry* **8**:2077-2089.

Zhu J, Ananthan S, Mactutus CF and Booze RM (2011) Recombinant human immunodeficiency virus-1 transactivator of transcription1-86 allosterically modulates dopamine transporter activity. *Synapse* **65**:1251-1254.

Zhu J, Ananthan S and Zhan CG (2018) The role of human dopamine transporter in NeuroAIDS. *Pharmacol Ther* **183**:78-89.

Zhu J, Apparsundaram S and Dwoskin LP (2009a) Nicotinic receptor activation increases [3H]dopamine uptake and cell surface expression of dopamine transporters in rat prefrontal cortex. *J Pharmacol Exp Ther* **328**:931-939.

Zhu J, Green T, Bardo MT and Dwoskin LP (2004) Environmental enrichment enhances sensitization to GBR 12935-induced activity and decreases dopamine transporter function in the medial prefrontal cortex. *Behav Brain Res* **148**:107-117.

Zhu J, Mactutus CF, Wallace DR and Booze RM (2009b) HIV-1 Tat protein-induced rapid and reversible decrease in [3H]dopamine uptake: dissociation of [3H]dopamine uptake and

[3H]2beta-carbomethoxy-3-beta-(4-fluorophenyl)tropane (WIN 35,428) binding in rat striatal synaptosomes. *J Pharmacol Exp Ther* **329**:1071-1083.

Zhu J and Reith ME (2008) Role of the dopamine transporter in the action of psychostimulants, nicotine, and other drugs of abuse. *CNS Neurol Disord Drug Targets* **7**:393-409.

Zhu J, Yuan Y, Midde NM, Gomez AM, Sun WL, Quizon PM and Zhan CG (2016) HIV-1 transgenic rats display an increase in [(3)H]dopamine uptake in the prefrontal cortex and striatum. *J Neurovirol* **22**:282-292.

Zou W, Kim BO, Zhou BY, Liu Y, Messing A and He JJ (2007) Protection against human immunodeficiency virus type 1 Tat neurotoxicity by Ginkgo biloba extract EGb 761 involving glial fibrillary acidic protein. *Am J Pathol* **171**:1923-1935.

JPET Fast Forward. Published on May 27, 2020 as DOI: 10.1124/jpet.120.266023
This article has not been copyedited and formatted. The final version may differ from this version.

Footnotes:

Research reported in this publication was supported by National Institutes of Health grants to JZ (R01DA035714 and R21DA041932), PIO (R01DA041513) and MTB (P50 DA05312).

JPET Fast Forward. Published on May 27, 2020 as DOI: 10.1124/jpet.120.266023
This article has not been copyedited and formatted. The final version may differ from this version.

Figure legends

Figure 1. Kinetic analysis of synaptosomal [^{3}H]DA uptake was determined in the PFC of iTat-tg mice following 7- or 14-day administration of saline or Dox. Synaptosomes were incubated with a range of mixed DA concentrations (0.1 – 5 µM, final concentration) containing a fixed concentration (12 nM) of [^{3}H]DA. The V_{max} and K_m values for [^{3}H]DA uptake via DAT (A and C) or NET (B and D) in the PFC of iTat-tg (iTat) mice following 7- (A and B) or 14- (C and D) day administration of saline or Dox were calculated using non-linear regression analysis with a one-site binding parameter and represent the means from five to seven independent experiments ± S.E.M. * $p < 0.05$, ** $p < 0.01$ compared to saline control group.

Figure 2. Analysis of plasmalemmal surface expression of DAT and NET was determined in the PFC of iTat-tg mice following 7-day administration of saline or Dox. Synaptosomes were incubated with sulfo-NHS-biotin and Pierce monomeric avidin beads and washed multiple times to isolate the DAT or NET, which was present on the plasmalemmal membrane. Top panels: representative immunoblots of total and biotinylated (Biotin) fraction of DAT (A) or NET (B) from the PFC of iTat-tg (iTat) mice from Dox-treated and saline (SAL) control groups. Calnexin was used as control protein. Bottom panels: the ratio of total or biotinylated DAT (A) or NET (B) immunoreactivity to calnexin immunoreactivity expressed as mean ± S.E.M. from five independent experiments.

Figure 3. Saturation binding of [^{3}H]WIN 35,428 or [^{3}H]Nisoxetine in the PFC of iTat-tg mice following 7- day administration of saline or Dox. For [^{3}H]WIN 35,428 binding to DAT, synaptosomes were incubated in assay buffer with one of six concentrations of [^{3}H]WIN 35,428 (1-30 nM, final concentration) and 1 µM desipramine on ice for 2 h. Nonspecific binding was determined in the presence of 10 µM cocaine. For [^{3}H]Nisoxetine binding to NET,

JPET Fast Forward. Published on May 27, 2020 as DOI: 10.1124/jpet.120.266023
This article has not been copyedited and formatted. The final version may differ from this version.

synaptosomes were incubated in assay buffer with one of six concentrations of nisoxetine (0.5-30 nM, final concentration) along with a fixed concentration of [^{3}H]Nisoxetine (3 nM) and 0.1 µM GBR12909 on ice for 2 h. Nonspecific binding was determined in the presence of 10 µM desipramine. The B_{max} and K_d values for [^{3}H]WIN 35,428 (A) or [^{3}H]Nisoxetine (B) binding to DAT or NET in the PFC of iTat-tg (iTat) mice following 7- day administration of saline or Dox were calculated using non-linear regression analysis with a one-site binding parameter and represent the means ± S.E.M. from five independent experiments. * $p < 0.05$, ** $p < 0.01$ compared to saline control group. DA turnover rate values were determined for DAT from (C) the V_{max} of [^{3}H]DA uptake (Figure 1A)/B_{max} of [^{3}H]WIN 35,428 binding and (D) the K_m/K_d of [^{3}H]DA uptake (Figure 1A)/B_{max} of [^{3}H]WIN 35,428 binding and for NET from (E) the V_{max} of [^{3}H]DA uptake (Figure 1B)/B_{max} of [^{3}H]Nisoxetine binding and (F) the K_m/K_d of [^{3}H]DA uptake (Figure 1B)/B_{max} of [^{3}H]Nisoxetine binding.

Figure 4. DA and dihydroxyphenylacetic acid (DOPAC) tissue content in the PFC and striatum of iTat-tg mice following 7-day administration of saline or Dox. Top panels: DA (A) and DOPAC (B) tissue content in the PFC of iTat-tg (iTat) mice from Dox-treated or saline (SAL) control groups. Bottom panels: DA (C) and DOPAC (D) tissue content in striatum (STR) of iTat-tg mice from Dox-treated or saline control groups. Data are expressed as ng/mg tissue (mean ± S.E.M.) from 5-6 mice per group. * $p < 0.05$, compared to saline control group.

Figure 5. Whole-cell patch clamp electrophysiology was performed in layer V pyramidal neurons of the prelimbic region of PFC in iTat-tg mice following 7-day administration of saline or Dox. Coronal slices (300 µm) containing the prelimbic cortex were cut with a Vibratome and incubated in an ice-cold artificial CSF (aCSF) solution at 32–34°C for 45 min and kept at 22–25°C thereafter, until transfer to the recording chamber. (A) Representative traces from iTat-tg mice treated with saline (iTat-Saline) and Dox (iTat-Dox) following hyperpolarizing (-200 pA) and

JPET Fast Forward. Published on May 27, 2020 as DOI: 10.1124/jpet.120.266023
This article has not been copyedited and formatted. The final version may differ from this version.

depolarizing (+200 pA) current steps. Summary of basal action potential frequency (B) and action potential frequency in response to acute application of DA (10 nM) or DA + GBR 12909 (100 nM) or DA + GBR 12909 + DMI (1 μM) of neurons from iTat-tg mice treated with saline (C) or Dox (D). * $p < 0.05$, n=15 and n=8 for saline and Dox treated mice, respectively.

JPET Fast Forward. Published on May 27, 2020 as DOI: 10.1124/jpet.120.266023
This article has not been copyedited and formatted. The final version may differ from this version.

Table 1. Kinetic properties of [^{3}H]DA uptake and [^{3}H]WIN 35,428 binding or [^{3}H]Nisoxetine binding in iTat-tg mice

			Striatum (DAT)		Hippocampus (NET)	
			V_{max} (pmol/min/mg)	K_m (nM)	V_{max} (pmol/min/mg)	K_m (nM)
Treatment duration	7-days	iTat-tg Saline	15.6 ± 1.4	97.3 ± 6.6	0.898 ± 0.12	102 ± 23
		iTat-tg Dox	15.6 ± 1.6	91.1 ± 3.4	0.926 ± 0.077	75.4 ± 14
	14-days	iTat-tg Saline	67.6 ± 8.5	140 ± 11	1.96 ± 0.19	122 ± 18
		iTat-tg Dox	68.4 ± 8.9	141 ± 10	1.86 ± 0.26	115 ± 24
			B_{max} pmol/mg	K_d (nM)	B_{max} pmol/mg	K_d (nM)
	7-days	iTat-tg Saline	22.9 ± 3.7	20.34 ± 5.3	0.611 ± 0.10	13.4 ± 3.3
		iTat-tg Dox	25.4 ± 5.4	18.3 ± 1.8	0.552 ± 0.096	15.4 ± 2.0

Data are expressed as mean ± S.E.M. values from five to seven independent experiments performed in duplicate.

JPET Fast Forward. Published on May 27, 2020 as DOI: 10.1124/jpet.120.266023
This article has not been copyedited and formatted. The final version may differ from this version.

Figure 1

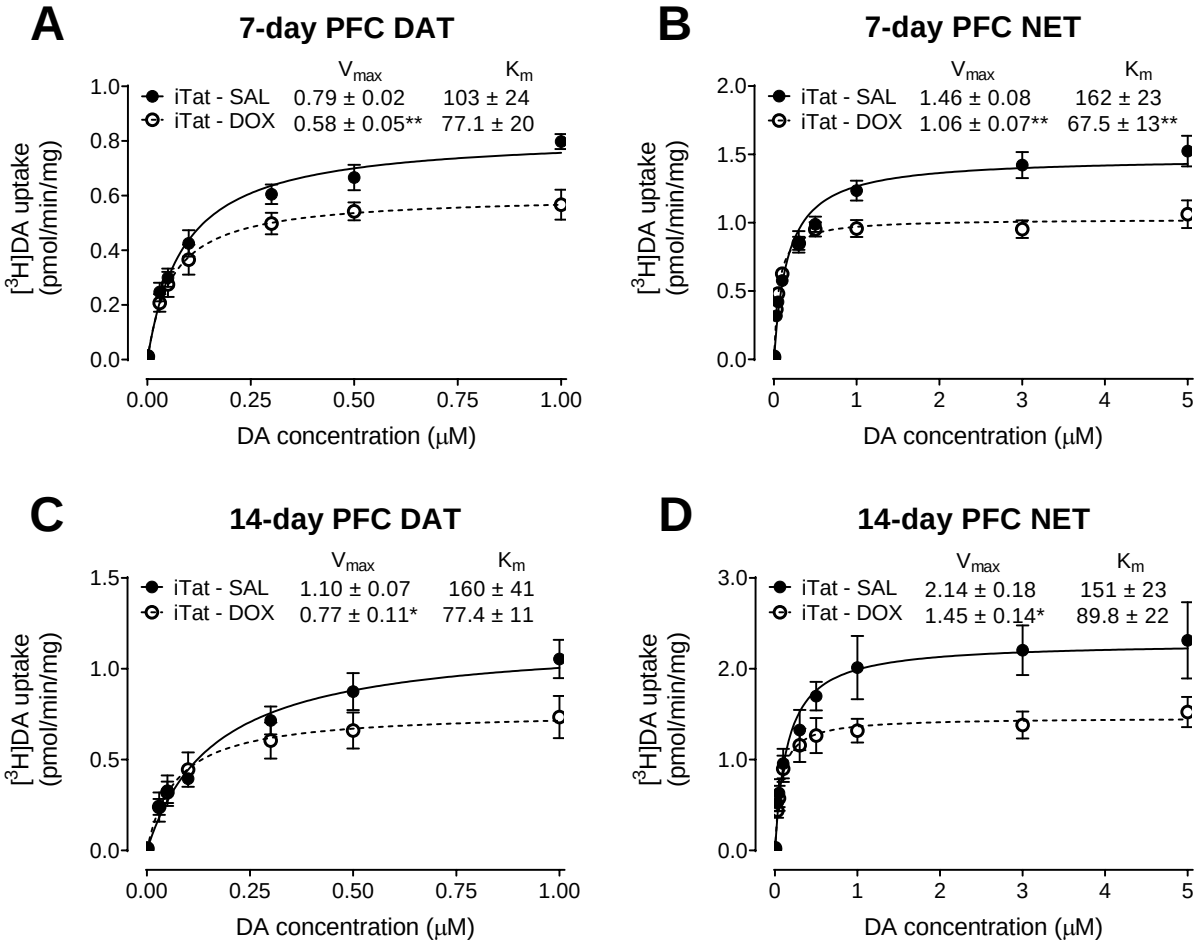

JPET Fast Forward. Published on May 27, 2020 as DOI: 10.1124/jpet.120.266023
This article has not been copyedited and formatted. The final version may differ from this version.

Figure 2

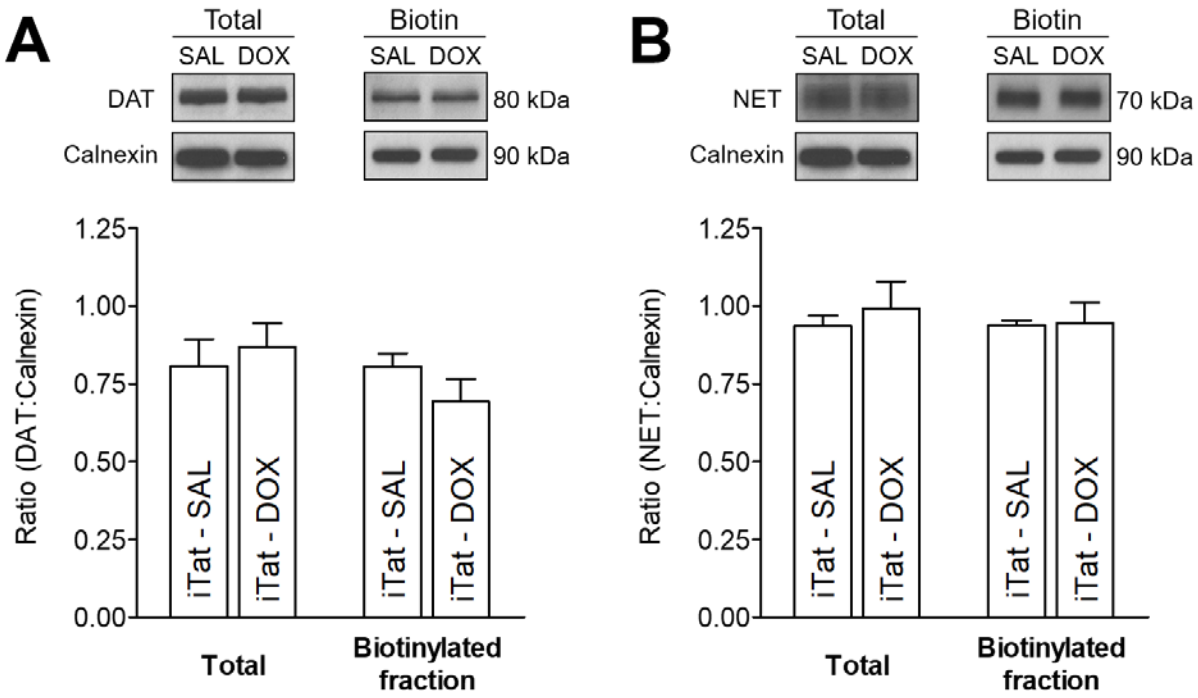

JPET Fast Forward. Published on May 27, 2020 as DOI: 10.1124/jpet.120.266023
This article has not been copyedited and formatted. The final version may differ from this version.

Figure 3

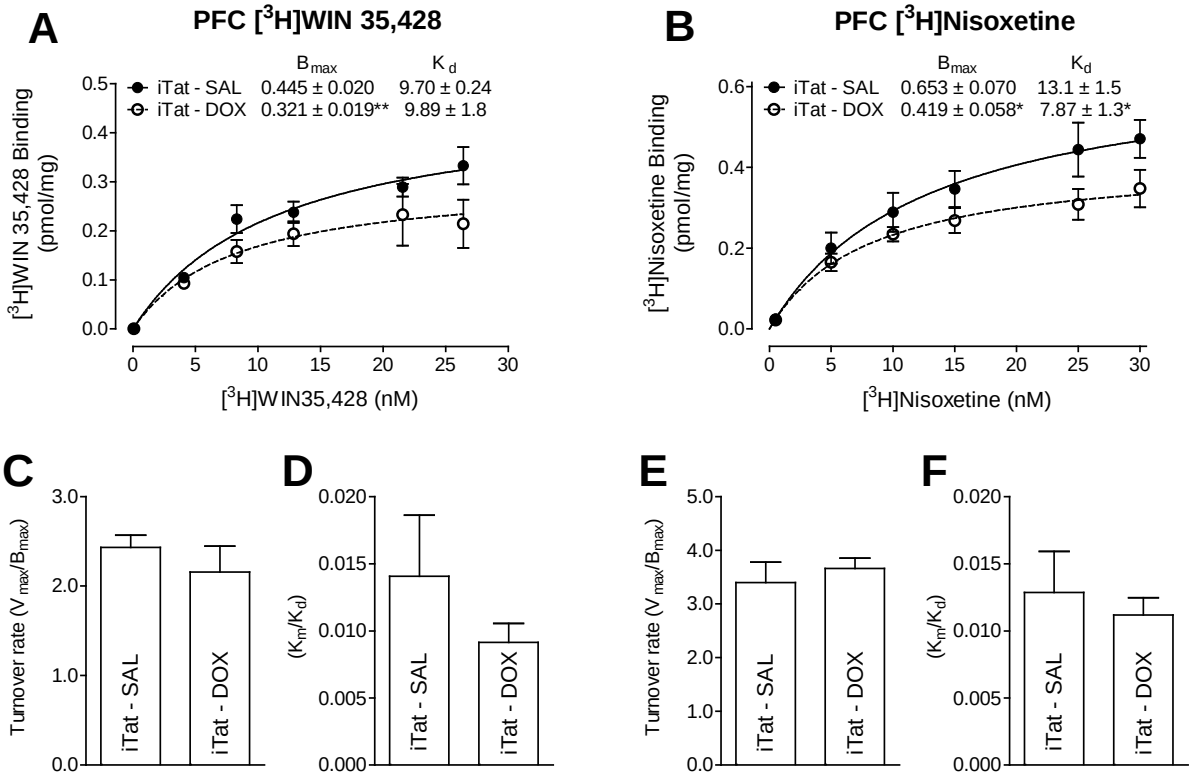

JPET Fast Forward. Published on May 27, 2020 as DOI: 10.1124/jpet.120.266023
This article has not been copyedited and formatted. The final version may differ from this version.

Figure 4

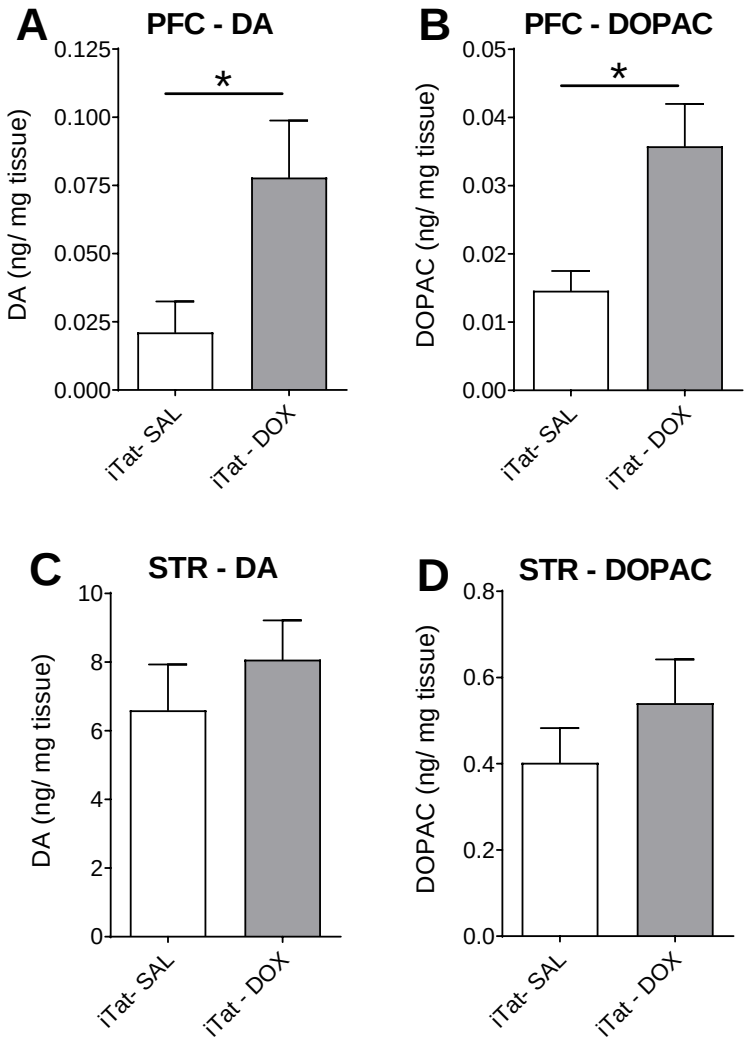

JPET Fast Forward. Published on May 27, 2020 as DOI: 10.1124/jpet.120.266023
This article has not been copyedited and formatted. The final version may differ from this version.

Figure 5

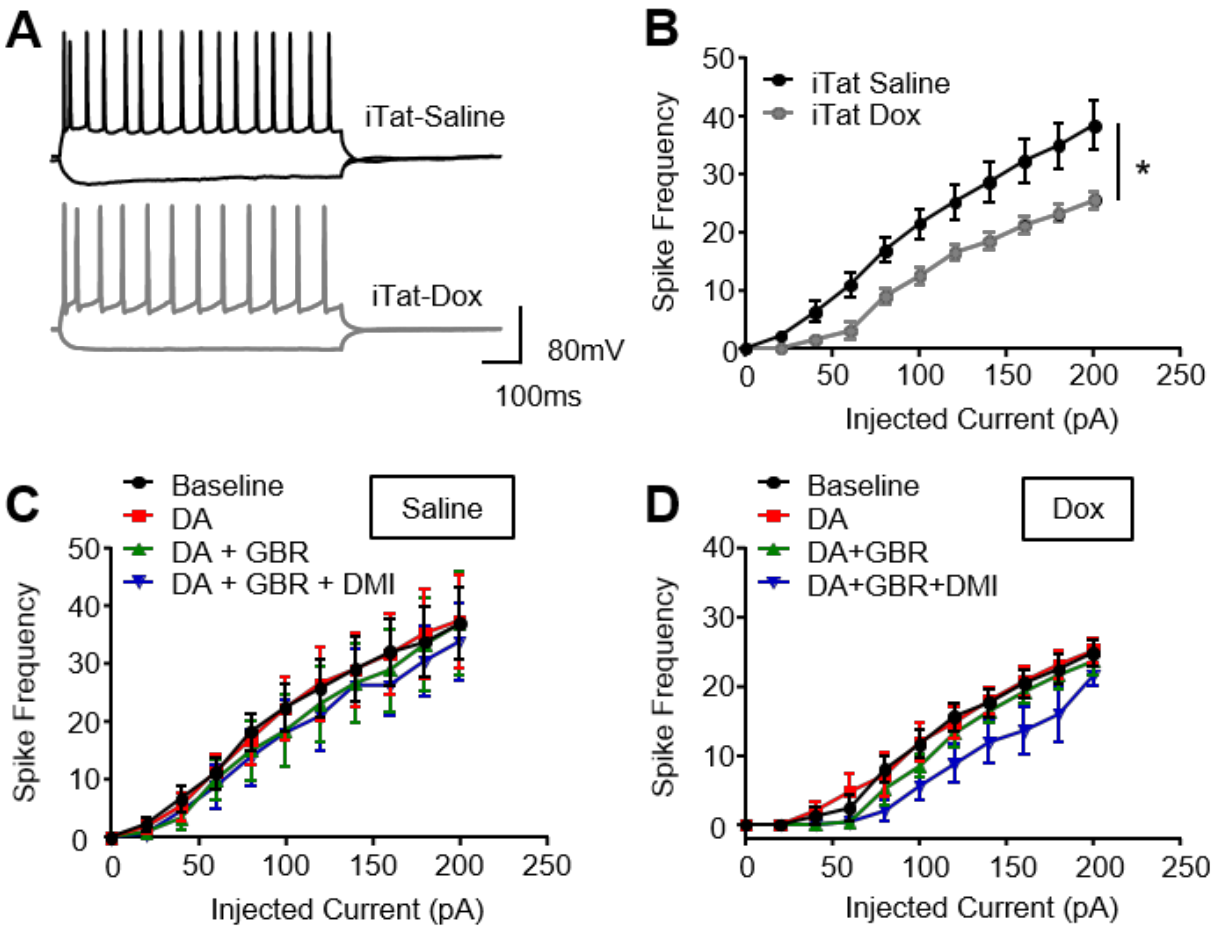

[^{3}H]Dopamine Uptake through the Dopamine and Norepinephrine Transporters is Decreased in the Prefrontal Cortex of Transgenic Mice Expressing HIV-1 Tat Protein

Matthew Strauss, Bernadette O'Donovan, Yizhi Ma, Ziyu Xiao, Steven Lin, Michael T. Bardo, Pavel I. Ortinski, Jay P. McLaughlin, and Jun Zhu*

MS, YM, ZX, SL, JZ - Department of Drug Discovery and Biomedical Sciences, College of Pharmacy, University of South Carolina, Columbia, SC 29208 USA

BO - Department of Physiology, Pharmacology and Neuroscience, School of Medicine, University of South Carolina, Columbia, SC 29208 USA

MB - Department Psychology, University of Kentucky, Lexington, KY 40536 USA

PO – Department of Neuroscience, University of Kentucky, Lexington, KY 40536, USA

JM - Department of Pharmacodynamics, College of Pharmacy, University of Florida, Gainesville, FL 32611 USA

The Journal of Pharmacology and Experimental Therapeutics (JPET Manuscript # 266023)

Supplemental Figure Legends

Supplemental Figure 1. Analysis of plasmalemmal surface expression of DAT and NET was determined in the striatum and hippocampus of iTat-tg mice following 7-day administration of saline or Dox. Synaptosomes were incubated with sulfo-NHS-biotin and Pierce monomeric avidin beads and washed multiple times to isolate the DAT or NET which was present on the plasmalemmal membrane. Top panels: representative immunoblots of the total and biotinylated (Biotin) fraction of DAT in the striatum (A) or NET in hippocampus (B) from iTat-tg mice from Dox-treated and saline (SAL) control groups. Calnexin was used as control protein. Bottom panels: the ratio of total or biotinylated DAT (A) and NET (B) immunoreactivity to calnexin immunoreactivity expressed as mean ± S.E.M. from five independent experiments.

Supplemental Figure 2. Analysis of plasmalemmal surface expression of DAT (in PFC and striatum) and NET (in PFC and hippocampus) was determined in C57BL/6J mice following 7-day administration of saline or Dox. Synaptosomes were incubated with sulfo-NHS-biotin and Pierce monomeric avidin beads and washed multiple times to isolate the DAT or NET which was present on the plasmalemmal membrane. Top panels: representative immunoblots for the total and biotinylated (Biotin) fraction of DAT in the PFC (A) and striatum (C) or NET in the PFC (B) and hippocampus (D) from C57BL/6J (C57) from Dox-treated and saline (SAL) control groups. Calnexin was used as control protein. Bottom panels: the ratio of total or biotinylated DAT or NET immunoreactivity to calnexin immunoreactivity (A-D) expressed as mean ± S.E.M. from 3-5 independent experiments.

Supplemental figure 3. DA and dihydroxyphenylacetic acid (DOPAC) tissue content in the PFC and striatum of G-tg mice following 7-day administration of saline or Dox. Top panels: DA (A) and DOPAC (B) tissue content in the PFC of G-tg mice from Dox-treated or saline (SAL) control

groups. Bottom panels: DA (C) and DOPAC (D) tissue content in striatum (STR) of G-tg mice from Dox-treated or saline (SAL) control groups. Data are expressed as ng/mg tissue (mean ± S.E.M.) from 5-6 independent experiments.

Supplemental figure 4. Whole-cell patch clamp electrophysiology was performed in layer V pyramidal neurons of the prelimbic region of PFC in C57BL/6J mice following 7-day administration of saline or Dox. Coronal slices (300 µm) containing the prelimbic cortex were cut with a Vibratome and incubated in an ice-cold artificial CSF (aCSF) solution at 32–34°C for 45 min and kept at 22–25°C thereafter, until transfer to the recording chamber. (A) Representative traces from C57BL/6J (C57) mice treated with saline (C57-Saline) and Dox (C57-Dox) following hyperpolarizing (-200 pA) and depolarizing (+200 pA) current steps. Summary of basal action potential frequency (B) and action potential frequency in response to acute application of DA (10 nM) or DA + GBR 12909 (100 nM) or DA + GBR 12909 + DMI (1 µM) of neurons from C57BL/6J mice treated with saline (C) or Dox (D).

Supplemental Figure 1

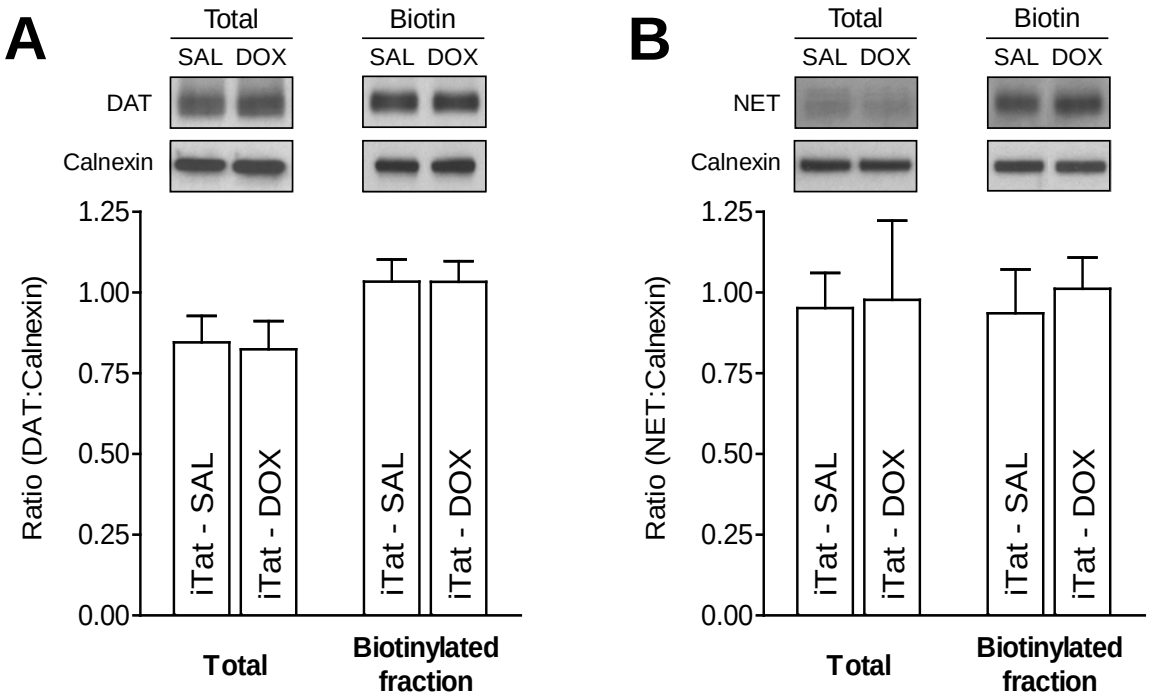

Supplemental Figure 2

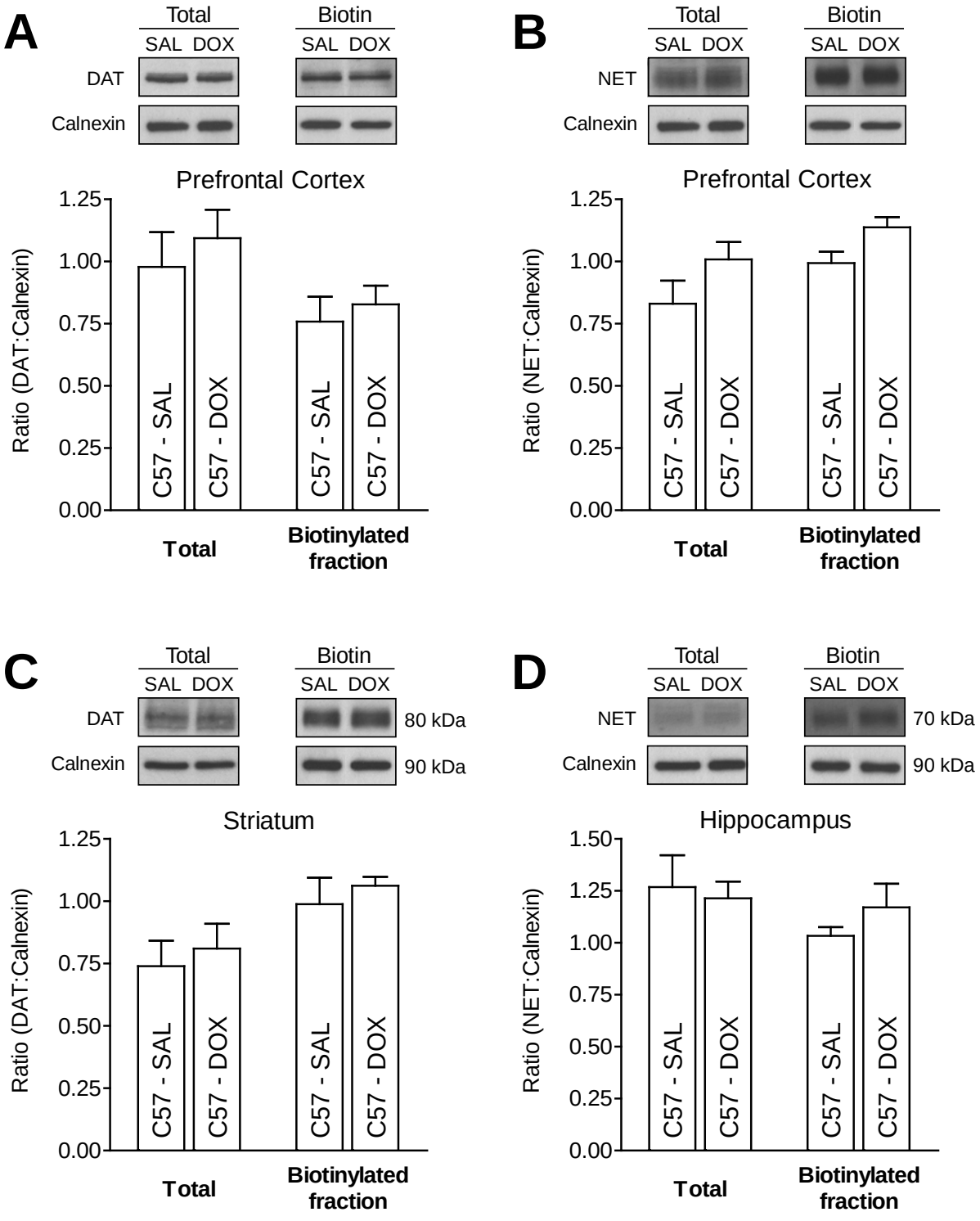

Supplemental Figure 3

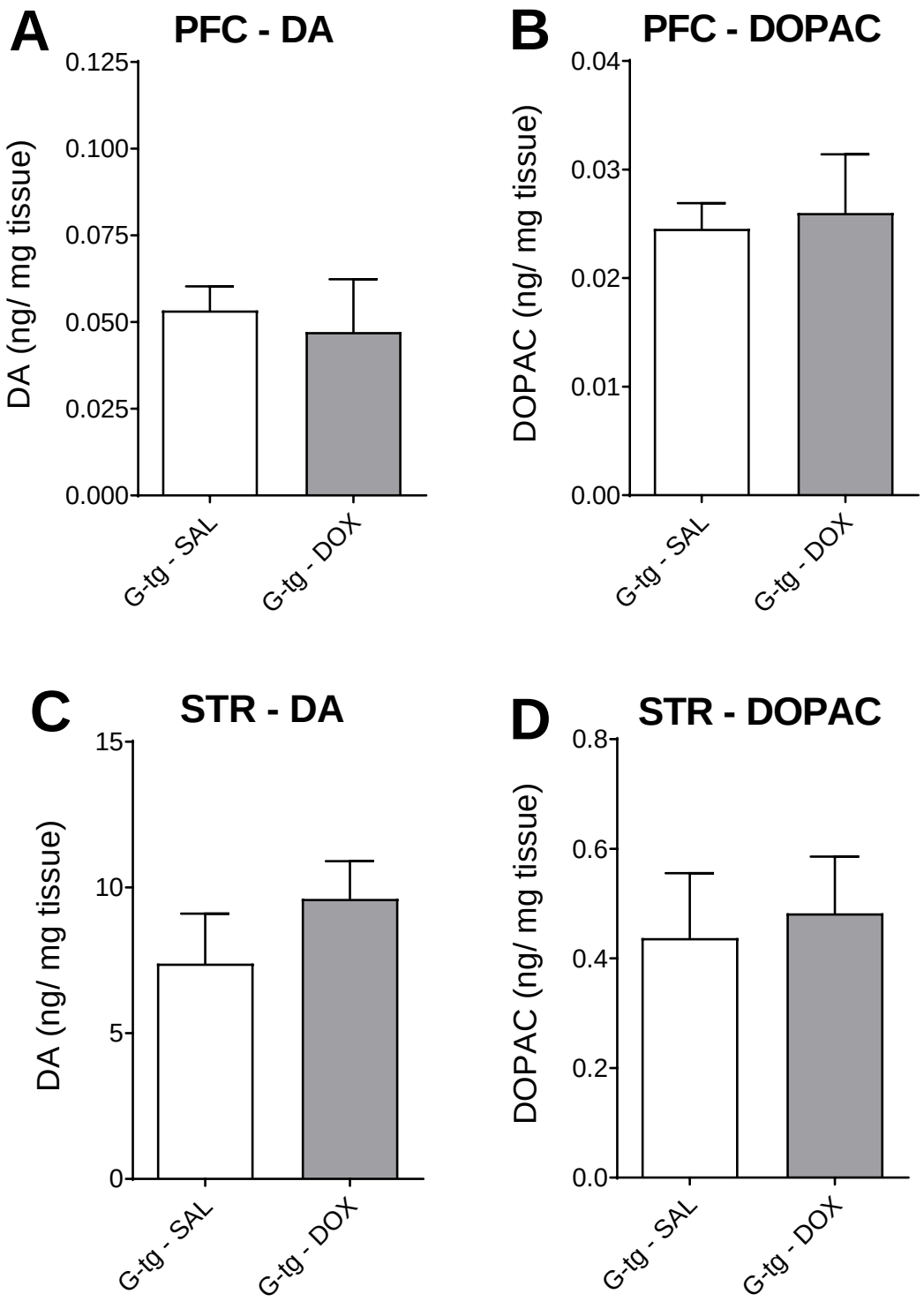

Supplemental Figure 4

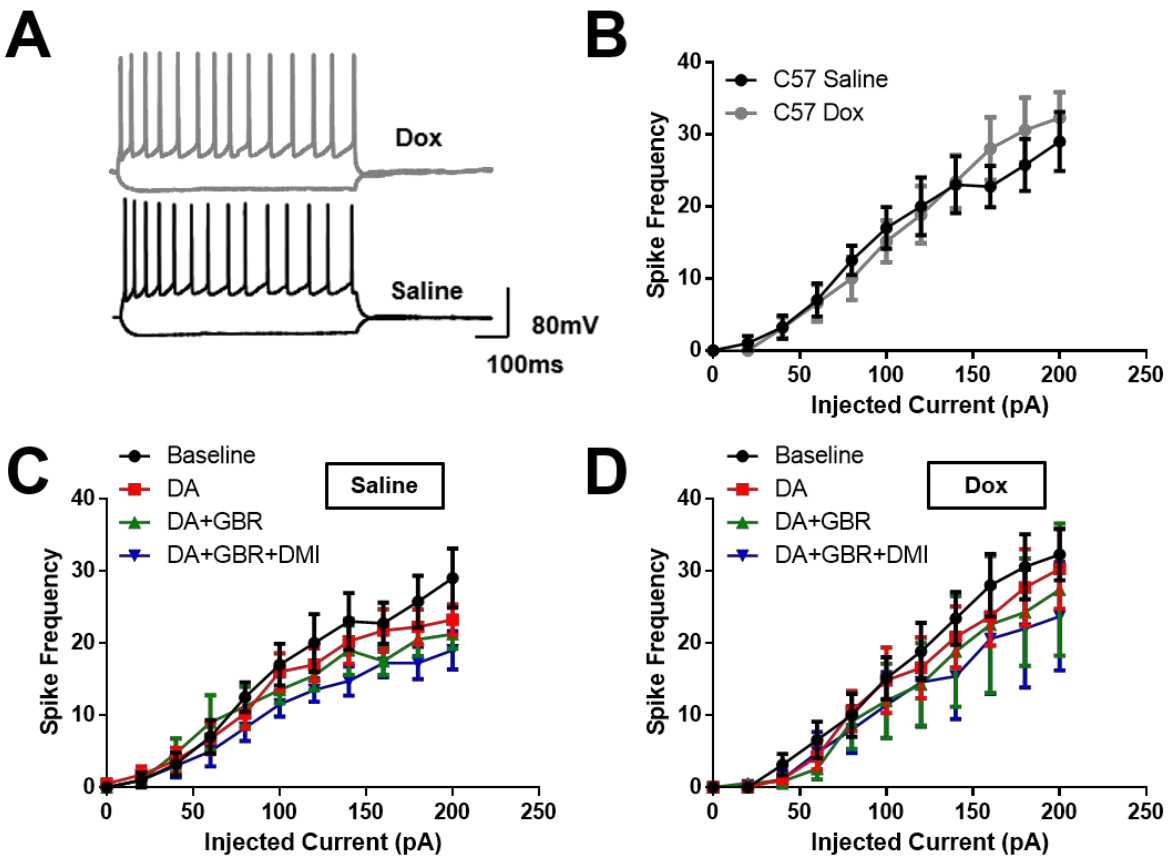

Supplemental Tables

Supplemental Table 1. Kinetic properties of [^{3}H]DA uptake and [^{3}H]WIN 35,428 binding for DAT in C57BL/6J mice

			Prefrontal cortex		Striatum	
			V_{max} (pmol/min/mg)	K_m (nM)	V_{max} (pmol/min/mg)	K_m (nM)
Treatment duration	7-days	C57 - Saline	0.590 ± 0.080	90.8 ± 16	15.1 ± 1.1	100 ± 12
		C57 - Dox	0.647 ± 0.044	77.6 ± 26	14.7 ± 1.2	103 ± 5.7
	14-days	C57 - Saline	0.685 ± 0.048	109 ± 10	51.9 ± 4.0	149 ± 7.5
		C57 - Dox	0.708 ± 0.11	84.3 ± 8.3	54.7 ± 5.5	154 ± 8.2
			B_{max} pmol/mg	K_d (nM)	B_{max} pmol/mg	K_d (nM)
	7-days	C57 - Saline	0.423 ± 0.19	9.02 ± 1.3	26.9 ± 3.5	14.6 ± 0.89
		C57 - Dox	0.395 ± 0.065	7.84 ± 1.5	29.9 ± 4.9	16.9 ± 2.1

Data are expressed as mean ± S.E.M. values from five to seven independent experiments performed in duplicate.

Supplemental Table 2. Kinetic properties of [^{3}H]DA uptake and [^{3}H]Nisoxetine binding for NET in C57BL/6J mice

			Prefrontal cortex		Hippocampus	
			V_{max} (pmol/min/mg)	K_m (nM)	V_{max} (pmol/min/mg)	K_m (nM)
Treatment duration	7-days	C57 - Saline	1.15 ± 0.063	158 ± 42	0.972 ± 0.047	86.0 ± 16
		C57 - Dox	1.14 ± 0.064	156 ± 35	0.962 ± 0.12	93.3 ± 18
	14-days	C57 - Saline	2.02 ± 0.25	92.2 ± 15	2.30 ± 0.29	86.5 ± 38
		C57 - Dox	1.98 ± 0.24	83.9 ± 17	2.26 ± 0.22	88.9 ± 28
			B_{max} pmol/mg	K_d (nM)	B_{max} pmol/mg	K_d (nM)
	7-days	C57 - Saline	0.553 ± 0.051	12.9 ± 3.2	0.636 ± 0.11	7.39 ± 0.72
		C57 - Dox	0.591 ± 0.12	11.0 ± 3.0	0.645 ± 0.13	8.59 ± 1.1

Data are expressed as mean ± S.E.M. values from five to seven independent experiments performed in duplicate.

Supplemental Table 3. Kinetic properties of [^{3}H]DA uptake via DAT in PFC and striatum or NET in PFC and hippocampus in G-tg mice following 7-day administration of saline or Dox

		Prefrontal cortex		Striatum	
		V_{max} (pmol/min/mg)	K_m (nM)	V_{max} (pmol/min/mg)	K_m (nM)
DAT	G-tg - Saline	0.343 ± 0.037	61.0 ± 18	33.3 ± 4.7	78.1 ± 5.3
	G-tg - Dox	0.317 ± 0.065	55.5 ± 17	32.3 ± 2.7	73.1 ± 1.4
		Prefrontal cortex		Hippocampus	
		V_{max} (pmol/min/mg)	K_m (nM)	V_{max} (pmol/min/mg)	K_m (nM)
NET	G-tg - Saline	0.945 ± 0.058	89.3 ± 23	1.39 ± 0.13	110 ± 10
	G-tg - Dox	1.09 ± 0.20	75.7 ± 2.5	1.41 ± 0.10	113 ± 23

Data are expressed as mean ± S.E.M. values from three independent experiments performed in duplicate.

Supplemental Table 4. Average age and total number of mice used for each experiment type by genotype and treatment.

	iTat-tg Saline	iTat-tg Dox	C57 Saline	C57 Dox	Total mice used
7-day [^{3}H]DA uptake	11.3 ± 0.41	10.8 ± 0.30	11.8 ± 0.11	12.0 ± 0.09	168
14-day [^{3}H]DA uptake	11.8 ± 0.34	11.2 ± 0.26	11.4 ± 0.24	11.4 ± 0.24	144
Surface Biotinylation	11.1 ± 0.14	11.1 ± 0.14	10.9 ± 0.15	10.9 ± 0.15	36
[^{3}H]WIN and [^{3}H]NXT binding	10.6 ± 0.28	10.3 ± 0.19	12.0 ± 0.27	12.0 ± 0.27	120
DA and DOPAC tissue content	11.9 ± 0.17	11.9 ± 0.17	12.6 ± 0.21 (G-tg mice)	12.6 ± 0.21 (G-tg mice)	24
Patch Clamp Ephys.	10.3 ± 0.44	10.4 ± 0.23	10.6 ± 0.30	11.0 ± 0.25	12

Age of mice is shown in weeks ± S.E.M.. Note that for several experiments the saline and dox groups are the same age; this is because they were tested simultaneously, and treatment was able to be distributed amongst littermates in these experiments. G-tg mice were used as an additional control for the 7-day [^{3}H]DA uptake with an average age of 11.4 ± 0.74 weeks for both saline and Dox treated groups.

Supplemental Table 5. Pearson's correlation coefficient of age versus experimental output

	PFC – DAT	STR – DAT	PFC – NET	HIP – NET
7-day [^{3}H]DA uptake (V_{max})	0.018	0.031	0.273	0.018
14-day [^{3}H]DA uptake (V_{max})	0.024	0.216	0.345	0.260
Biotinylation – Total	-0.433	-0.101	-0.048	-0.516
Biotinylation – Surface	-0.258	-0.040	-0.200	0.193
[^{3}H]WIN and [^{3}H]NXT binding (B_{max})	-0.166	0.445	-0.020	0.423
	PFC – DA	PFC – DOPAC	STR – DA	STR – DOPAC
DA and DOPAC tissue content	-0.275	0.192	-0.365	-0.166

Pearson's correlation coefficient was determined using Graphpad Prism 8 software. Age was used as the x-axis and experimental output was used for the y-axis. No significant correlations were found between age and any experimental output.

[^{3}H]Dopamine Uptake through the Dopamine and Norepinephrine Transporters is Decreased in the Prefrontal Cortex of Transgenic Mice Expressing HIV-1 Tat Protein

Matthew Strauss, Bernadette O'Donovan, Yizhi Ma, Ziyu Xiao, Steven Lin, Michael T. Bardo, Pavel I. Ortinski, Jay P. McLaughlin, and Jun Zhu*

MS, YM, ZX, SL, JZ - Department of Drug Discovery and Biomedical Sciences, College of Pharmacy, University of South Carolina, Columbia, SC 29208 USA

BO - Department of Physiology, Pharmacology and Neuroscience, School of Medicine, University of South Carolina, Columbia, SC 29208 USA

MB - Department Psychology, University of Kentucky, Lexington, KY 40536 USA

PO – Department of Neuroscience, University of Kentucky, Lexington, KY 40536, USA

JM - Department of Pharmacodynamics, College of Pharmacy, University of Florida, Gainesville, FL 32611 USA

The Journal of Pharmacology and Experimental Therapeutics (JPET Manuscript # 266023)

Primary antibody: 1:500 (Goat anti-DAT Santa Cruz, C-20, SC-1433)
Secondary antibody: 1:10,000 (anti-goat-HRP 305-035-045, Jackson)

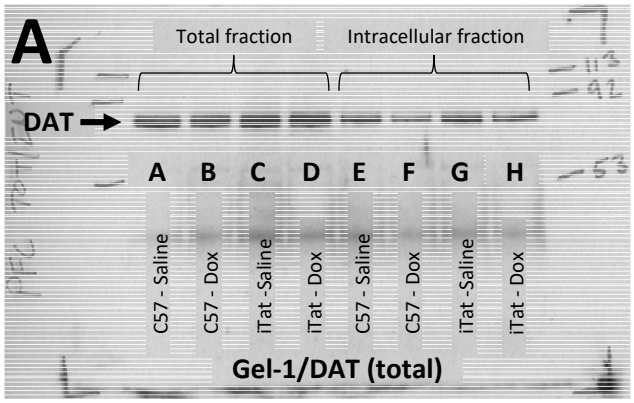

Primary antibody: 1:5,000 (Mouse anti-NET Mab tech, 05-1, NET05-1)
Secondary antibody: 1:10,000 (anti-mouse-HRP 7076S, Cell Signaling)

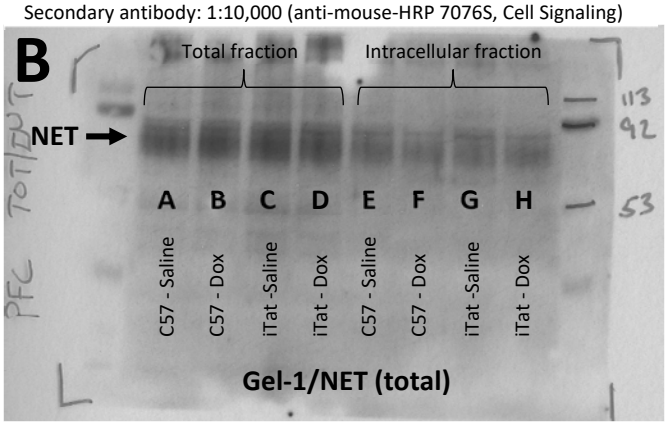

Primary antibody: 1:10,000 (Rabbit anti-Calnexin, H70, Santa Cruz, SC-11397)
Secondary antibody: 1:20,000 (anti-rabbit-HRP 111-035-144, Jackson)

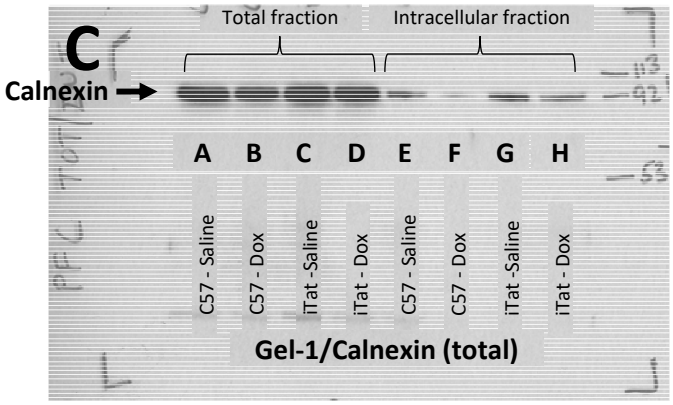

Representative immunoblots for total DAT (A), NET (B), and Calnexin (C) in C57 or iTat mice treated with saline or dox. Total and intracellular DAT (A), NET (B), and Calnexin (C) expression in C57 and iTat mice following 7-days of saline or dox treatment. The total and intracellular fractions were prepared and loaded as described in the methods section under the biotinylation and western blot heading. The membrane was first probed using the C-20 anti-DAT antibody (A), then stripped using Restore™ Western Blot Stripping Buffer (ThermoFisher, cat# 21059), and re-probed with NET05-1 anti-NET antibody (B). The same membrane was then stripped again and re-probed with H70 anti-calnexin antibody (C) to monitor protein loading between all lanes. Lanes C and D from panel A are shown in Figure 2A as total DAT fraction, and lanes C and D from panel B are shown in Figure 2B as total NET fraction. Lanes C and D from panel C are shown as the loading control for both total DAT (Figure 2A) and NET (Figure 2B) as the same sample was used to determine the expression of both proteins. Lanes A and B from all panels were used in supplemental Figure 2A and 2B in an identical manner.

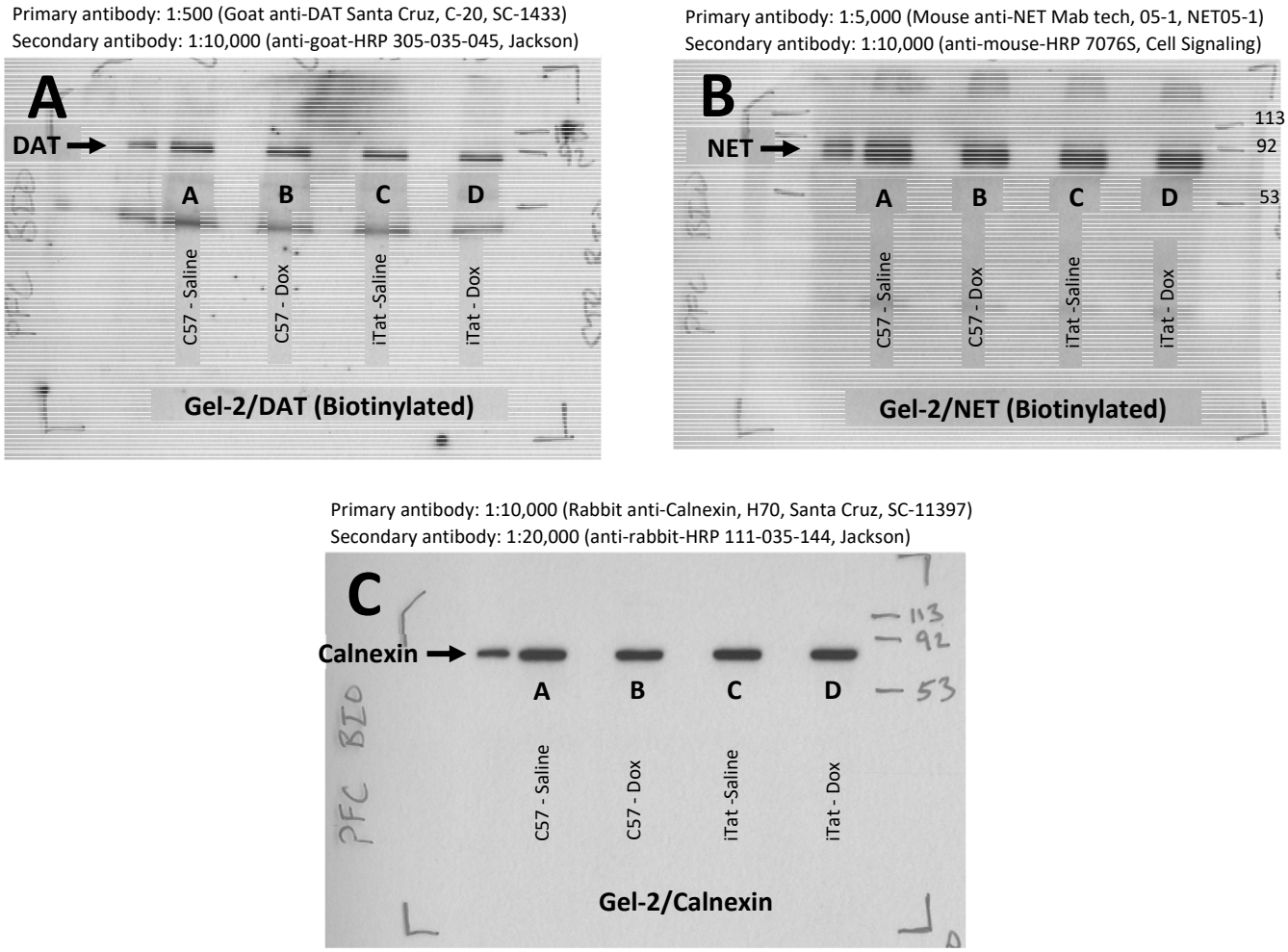

Representative immunoblots for biotinylated DAT (A), NET (B), and Calnexin (C) in C57 or iTat mice treated with saline or dox. Biotinylated DAT (A), NET (B), and Calnexin (C) expression in C57 and iTat mice following 7-days of saline or dox treatment. The biotinylated fraction was prepared and loaded as described in the methods section under the biotinylation and western blot heading. The membrane was first probed using the C-20 anti-DAT antibody (A), then stripped using Restore™ Western Blot Stripping Buffer (ThermoFisher, cat# 21059), and re-probed with NET05-1 anti-NET antibody (B). The same membrane was then stripped again and re-probed with H70 anti-calnexin antibody (C) to monitor protein loading between all lanes. Lanes C and D from panel A are shown in Figure 2A as biotinylated DAT fraction, and lanes C and D from panel B are shown in Figure 2B as biotinylated NET fraction. Lanes C and D from panel C are shown as the loading control for both biotinylated DAT (Figure 2A) and NET (Figure 2B) as the same sample was used to determine the expression of both proteins. Lanes A and B from all panels were used in supplemental Figure 2A and 2B in an identical manner.